ELEMENTA
Science of the Anthropocene

Alexander, MA, et al. 2018 Projected sea surface temperatures over the 21st century: Changes in the mean, variability and extremes for large marine ecosystem regions of Northern Oceans. *Elem Sci Anth,* 6: 9. DOI: https://doi.org/10.1525/elementa.191

RESEARCH ARTICLE

Projected sea surface temperatures over the 21st century: Changes in the mean, variability and extremes for large marine ecosystem regions of Northern Oceans

Michael A. Alexander*, James D. Scott*,†, Kevin D. Friedland‡, Katherine E. Mills§, Janet A. Nye‖, Andrew J. Pershing§ and Andrew C. Thomas¶

Global climate models were used to assess changes in the mean, variability and extreme sea surface temperatures (SSTs) in northern oceans with a focus on large marine ecosystems (LMEs) adjacent to North America, Europe, and the Arctic Ocean. Results were obtained from 26 models in the Community Model Intercomparison Project Phase 5 (CMIP5) archive and 30 simulations from the National Center for Atmospheric Research Large Ensemble Community Project (CESM-LENS). All of the simulations used the observed greenhouse gas concentrations for 1976–2005 and the RCP8.5 "business as usual" scenario for greenhouse gases through the remainder of the 21st century. In general, differences between models are substantially larger than among the simulations in the CESM-LENS, indicating that the SST changes are more strongly affected by model formulation than internal climate variability. The annual SST trends over 1976–2099 in the 18 LMEs examined here are all positive ranging from 0.05 to 0.5°C decade^{-1}. SST changes by the end of the 21st century are primarily due to a positive shift in the mean with only modest changes in the variability in most LMEs, resulting in a substantial increase in warm extremes and decrease in cold extremes. The shift in the mean is so large that in many regions SSTs during 2070–2099 will *always* be warmer than the *warmest year* during 1976–2005. The SST trends are generally stronger in summer than in winter, as greenhouse gas heating is integrated over a much shallower climatological mixed layer depth in summer than in winter, which amplifies the seasonal cycle of SST over the 21st century. In the Arctic, the mean SST and its variability increases substantially during summer, when it is ice free, but not during winter when a thin layer of ice reforms and SSTs remain near the freezing point.

Keywords: Sea surface temperature; Mixed layer depth; Climate change; Global climate models; Extremes; Marine ecosystems

Introduction

The burning of fossil fuels and the resulting input of CO_2 and other greenhouse gases into the atmosphere has already warmed the planet and will have a profound impact on the Earth, including the oceans, over the 21st century. The effects of increasing ocean temperatures, including rising sea levels, enhanced ocean stratification, decreased sea-ice extent, and altered patterns of ocean circulation (e.g., IPCC, 2013), will have substantial impacts on fish and marine ecosystems (e.g., Doney et al., 2012; Brander 2010, 2013; Hollowed et al., 2013). In this study, we primarily focus on changes in the mean, variability and extreme sea surface temperatures (SSTs), with additional analyses of mixed layer depth (MLD), to better understand the changes in SSTs.

SST is a key variable in the climate system, regulating thermal and dynamical interactions between the ocean and atmosphere. Compared to most other ocean variables, SST is well sampled over the open ocean, especially since satellite measurements became available in 1979. While SSTs are generally available from archives of climate model simulations, the availability of temperature and other variables as a function of depth is much more restricted. In addition, temperature controls all physiological processes in marine organisms (Fry 1971, Rivkin and Legendre, 2001, Deutsch et al., 2015) and as such, SSTs are often a leading indicator and/or important driver of marine ecosystem fluctuations (Mueter et al., 2009; Drinkwater et

* NOAA/Earth System Research Laboratory, Physical Science Division, Boulder, Colorado, US
† CIRES, University of Colorado, Boulder, Colorado, US
‡ National Marine Fisheries Service, Narragansett, Rhode Island, US
§ Gulf of Maine Research Institute, Portland, Maine, US
‖ School of Marine and Atmospheric Sciences, Stony Brook University, Stony Brook, New York, US
¶ School of Marine Sciences, University of Maine, Orono, Maine, US
Corresponding author: Michael A. Alexander (Michael.Alexander@noaa.gov)

al., 2010; Ottersen et al., 2010), including fish distributions (e.g., Nye et al., 2009; Block et al., 2011; Pinsky et al., 2013), fish recruitment (e.g., Planque and Fredou, 1999; Hunt et al., 2011; Kristiansen et al., 2011) and biodiversity (Edwards and Richardson, 2004; Tittensor et al., 2010). Even bottom-dwelling marine organisms are greatly influenced by changes in SST as most spend at least part of their life cycle either as pelagic larvae or depend on food sources that are affected by SST. Furthermore, in the temperate marine ecosystems on which we focused, the water column is mixed seasonally such that changes in SST are transmitted to deeper waters.

Observations indicate that the mean sea surface temperature (SST) of the global ocean has risen by ~0.06°C per decade from 1901–2012 and ~0.095°C per decade from 1979–2012 (Hartmann et al., 2013). Observed SST trends (1900–2008) indicate that warming occurred over most of the global oceans with the exception of a small portion of the Atlantic to the south of Greenland and some areas in the equatorial Pacific, although there is disagreement among data sets due to the paucity of observations in the tropical Pacific Ocean (Deser et al., 2010). The ensemble mean sea surface temperatures from climate models within the Coupled Model Intercomparison Project (CMIP3, Meehl et al., 2007, and CMIP5, Taylor et al., 2012) track the observed changes in globally averaged SST remarkably well over the 20th century, and the simulated warming is consistent with the observed trends over ~70% of the oceans (Knutson et al., 2013).

While basin-wide changes in the ocean are expected, it is critical to examine temperature changes along continental margins, which supply more than 75% of the world's marine fish catch (IOC-UNESCO and UNEP, 2016). Approximately, 72% of coastal areas experienced significant increases in SST at an overall rate of 0.25°C per decade from 1982 to 2010 (Lima and Wethey, 2012). Large Marine Ecosystems (LMEs) are defined as "coherent ocean areas generally along continental margins whose ecological systems are characterized by similarities in bathymetry, hydrography, and biological productivity" (Sherman and Alexander, 1986; Sherman and Duda, 1999). LMEs were developed by the US National Oceanic and Atmospheric Administration (NOAA) to further ecosystem-based management and identify ocean regions for conservation. Of the 64 LME regions examined by Belkin (2009), all but three exhibited warming from 1982–2006 with many of the regions with the strongest warming occurring at high latitudes in the North Atlantic.

Changing ocean temperatures, including seasonal differences in warming trends, may influence the behavior, growth, reproduction and survival of marine species. For example, based on monthly SST data, Edwards and Richardson (2004) found that the marine pelagic community response to climate change varied over the seasonal cycle, leading to a mismatch between trophic levels and functional groups. Yet, the seasonal cycle of temperature trends has been explored in only a few studies. Warming of SSTs was more intense in summer and fall than in winter and spring off the northeast coast of the United States (Friedland and Hare, 2007; Thomas et al., 2017) and in the Caribbean (Chollett et al., 2012). In the Mediterranean, the observed warming trend was greatest in spring and lowest in winter, while the CMIP5 models project stronger warming in summer (López García and Belmonte, 2011; Shaltout and Omested, 2014).

Climate change may not only manifest in mean SST trends but also in changes in the variability and extremes. Climate change can impact extremes simply due to a shift in the mean state, e.g., with very high (low) temperatures becoming more (less) frequent as the mean climate warms. However, increasing greenhouse gases may also alter the variability and the overall probability distribution of temperatures and other variables in the climate system, making extreme events even more or less extreme. For example, the spread of anomalies about the mean can become larger, e.g., as indicated by an increase in the standard deviation, or the distribution can change shape, e.g., by becoming more skewed. Observations indicate that surface air temperatures over land have been becoming more extreme, primarily due to a shift in the mean towards higher temperatures (Ballester et al., 2009; Simolo et al., 2011; Weaver et al., 2014; Thompson et al., 2015), but with both increases and decreases in the standard deviation and/or skewness in some regions (e.g., Donat and Alexander, 2012; Fischer and Schär 2009; Screen, 2014; Schneider et al., 2015). Changes in precipitation are likely to involve large changes in the probability distribution, with extreme precipitation events generally projected to rise (e.g., Kharin et al., 2007; IPCC, 2012; Kunkel et al., 2013), but it is not clear that the number or intensity of heavy precipitation events will increase in all locations or during all seasons (Alexander et al., 2013; Mahoney et al., 2013; Sardeshmukh et al., 2015; Huang and Ullrich, 2017). Changes in the distribution of other variables, including ocean temperatures, have received less attention and may exhibit different distribution changes than temperature or precipitation over land.

Most research on climate extremes has focused on land, including studies of heat waves, heavy precipitation events, droughts, and floods (e.g., IPCC, 2012). Extreme conditions, however, also occur in the world oceans (Hobday et al., 2016) and there is a growing appreciation that extremes strongly influence population dynamics and biogeography of many organisms (Portner et al., 2001; Lynch et al., 2014). Recent studies have explored periods with very warm SSTs or "ocean heat waves" in the northwest Atlantic (Mills et al., 2013; Chen et al., 2014, 2015), Northern Hemisphere oceans (Scannell et al., 2016), Mediterranean Sea (Black et al., 2004; Olita et al., 2007), off the coast of western Australia (Pearce and Feng, 2013; Wernberg et al., 2013), and over global coastal regions (Lima and Wethey, 2012). Significant negative effects on living marine resources and marine ecosystems were observed during some of these extreme periods (Mills et al., 2013; Wernberg et al., 2013; Pershing et al., 2015; Caputi et al., 2016). Over the 21st century, changes in extreme SSTs will vary by region due to several factors, including internal climate variability and potential changes in ocean circulation, sea ice, stratification and ocean mixed layer depth (MLD).

One metric of a changing climate that incorporates changes in both the mean and extremes is the time at which a future climate permanently departs from the climate of the past. Diffenbaugh and Scherer (2011) defined this "time of emergence" as the year when the coolest warm-season of the 21st century is hotter than the hottest warm-season of the late 20th century. Using climate model simulations from the CMIP3 archive, Diffenbaugh and Scherer found that surface air temperature in many regions of the globe will likely exceed the bounds of the 20th century over the next four decades, with the most rapid emergence occurring in the tropics where the variability is low. A similar analysis conducted by Mora et al. (2013), based on the CMIP5, archive confirmed the general findings of Diffenbaugh and Scherer. They also examined the impact of changing air and ocean temperatures on biological hotspots and found that most marine hotspots will experience unprecedented warmth by the middle of the 21st century.

The surface layer of the ocean is often well mixed, and changes in the mixed layer depth affect SSTs. In addition to ocean temperatures, MLD variability affects the ocean's chemistry and biology, by influencing the amount of nutrients near the surface and the period of time phytoplankton remain within the euphotic zone. Over much of the extratropical oceans the MLD exhibits a large seasonal cycle: strong winds and convective mixing due to surface cooling, plus the ejection of salt during ice formation in polar regions, deepen the mixed layer in winter, while heating by solar radiation and light winds reduce mixing in summer. Air-sea heat fluxes are integrated over the mixed layer, with the resulting temperature change inversely proportional to the MLD. Thus, greenhouse gas-induced heating from the atmosphere that is mixed over a shallower surface layer in summer than in winter could result in stronger positive SST trends during the warm season, especially where the climatological seasonal differences in the MLD are large. Climate change is also likely to alter the MLD and thus can influence both temperature trends and variability. Based on models in the CMIP3 archive, Jang et al. (2011) found that the MLD decreased over most of the North Pacific between 1980–1999 and 2080–2999 during winter. However, future MLD changes over the remainder of the oceans, including the North Atlantic, have yet to be evaluated.

In this study, we used fields from global climate models to investigate how climate change affects the mean, variability, extremes, and time of emergence of SST anomalies in select LMEs. The seasonal variability and change in MLD were explored, focusing on their impacts on SSTs: we hypothesized that ecosystems with shallower MLDs would exhibit greater surface warming. We used simulations from a large number of models in the CMIP5 archive and from a large ensemble of runs from a single climate model initialized with different atmospheric states to examine the spread in the results due to intrinsic climate variability (i.e., changes due to interactions within the climate system). Given the focus of this Special Feature on the effects of climate changes on fish stocks in the Northern Hemisphere, particularly in the northeast Atlantic and around the United States, we examined maps encompassing the eastern North Pacific, Arctic Ocean and the North Atlantic and performed regional analyses in these ocean basins.

Models, data and analysis methods

While marine heat waves have begun to be studied using daily SST data (e.g., Hobday et al., 2016) several previous studies of warm SST extremes have used monthly data including Bond et al. (2015) and Scannel et al. (2016). An analysis of observed daily and monthly SST variability indicated that the variability on daily time scales was approximately 10–30% higher over most of the North Atlantic and Pacific with values reaching 50% in the Gulf Stream (not shown). However, monthly SST values are appropriate for the spatial scales we have analyzed in this study, as extreme daily anomalies are more likely to be smaller in scale than the LMEs. In addition, mobile animals can avoid stressful conditions by moving laterally or vertically and thus be able to cope with high temperatures over a few days but could experience much greater stress if the abnormal heating last a month or more. Thus, our analyses were performed using monthly averaged output from two different sets of model experiments and a gridded, observationally-based, SST data set.

CMIP 5

CMIP5 provided a framework for coordinated climate change experiments that were used extensively in the Intergovernmental Panel on Climate Change Fifth Assessment Report (IPCC AR5; IPCC, 2013). The CMIP5 archive contains a collection of global climate and earth system model simulations from more than 20 different research centers around the world, some of which have developed more than one model. Climate models have four main components: atmosphere, ocean, land and sea ice. CMIP5 also includes earth system models, which in addition to the four physical components also include chemistry and biology. Here we have used one ensemble member from 26 models in the CMIP5 archive (listed in supplemental Table S1), 11 of which are earth system models. The highest horizontal resolution of the ocean component of the CMIP5 models is 0.5° latitude (lat) × 0.5° longitude (lon) and the lowest is 2.0° lat × 2.5° lon, but most models have resolutions between 0.5°–1.0° lat and 1.0°–1.5° lon. The "historical" simulations are initiated in 1860 and extend to 2005 based on climate forcings (i.e., changes in greenhouse gases – including CO_2, volcanic effects, solar output, and land use) derived from observations. Future changes in greenhouse gases (starting in 2006) are based on the Representative Concentration Pathways (RCP). Here we have examined the RCP8.5 "business as usual" scenario in which the radiative forcing increases by 8.5 Wm^{-2} by 2100 corresponding to a CO_2 concentration of ~940 p.p.m. (Meinshausen et al., 2011; van Vuuren et al., 2011). We chose to do an in-depth analysis of one scenario with multiple models rather than a more cursory examination of multiple scenarios. RCP8.5 has the greatest increase in greenhouse gases of the scenarios used in the IPCC AR5 and thus should have the greatest signal-to-noise ratio

and indicate the potential for the greatest changes in extremes. In addition, actual greenhouse gas emissions have mostly closely matched RCP8.5 of all of the AR5 scenarios since their initiation in 2005 (Sanford et al., 2014).

CESM-LENS

Most climate change simulations have been conducted using only one or just a few (<5) ensemble members. However, due to the chaotic nature of the climate system, small differences in initial conditions at the start of model integrations will result in diverse climate trajectories over time. In the atmosphere, very small differences can grow rapidly resulting in dissimilar states after just a few weeks. Within a decade the ocean, ice and land also evolve differently, as a result of internal variability in the climate system. Thus, differences in the CMIP5 simulations can arise due to internal variability in addition to differences in the model formulations. Averaging a large number of simulations performed using the same model and the same external forcing but different initial conditions can provide a robust estimate of the climate change signal, where variability unrelated to the forcing is obtained from the spread among the simulations, avoiding differences in model formulation as a contributor to the spread. In this unique experimental design, the climate change signal is well characterized by the ensemble mean, while the internal climate variability is represented by the spread among simulations (Deser et al., 2012a, 2012b, 2014).

To evaluate the relative contribution of intrinsic climate variability to SST changes over the 21st century we used 30 simulations conducted as part of the Community Earth System Model large ensemble project (CESM-LENS; Kay et al., 2015). CESM (version 1; Hurrell et al., 2013) is a global earth system model developed at the National Center for Atmospheric Research (NCAR). All simulations in CESM-LENS use the same historical forcing from 1920 to 2005 and then the forcing based on the RCP 8.5 scenario from 2006 to 2100. The spread in the 30 ensemble members was generated by round-off level differences in their initial air temperature fields (on the order of 10^{-14} K). The atmosphere and land models in CESM have a horizontal resolution of about 1°. The ocean model has 60 vertical levels, where the layer thickness varies from 10 m near the surface to 250 m at depth. CESM1 was ranked as a top-performing model in CMIP5 by Knutti et al. (2013) and its climatic variability is similar to that in nature (Deser et al., 2017).

SST observations

For the analyses where model SSTs are compared with observations, we have used observations from the Hadley Center Ice-SST (HadISST1; Rayner et al., 2003) data set. The data set extends from 1870 to the present and is available on a 1° lat × 1° lon grid.

MLD

Mixed layer depth (MLD) was not available from all models in the CMIP5 archive, and the modeling centers that did provide MLD used different methods to estimate it. In addition, daily temperature, salinity, and density profiles were not archived. Thus, for CMIP5, we estimated MLDs based on monthly potential density data using the same threshold criteria as Suga et al. (2004), where the MLD is the depth at which the density exceeds the surface layer density by 0.125 kg m^{-3}. MLD in the CESM-LENS is based on daily MLD values estimated from the maximum buoyancy gradient (Large et al., 1997), which were subsequently monthly averaged. The different methodologies used to estimate MLD, in addition to different model physics, can result in regional MLD differences between CMIP5 and CESM-LENS.

Analysis methods

The SST was obtained from the ocean component of the CMIP5 and CESM-LENS models. We have interpolated all model fields to a 1° lat × 1° lon grid prior to performing any calculations in order to compare results between models and compute an ensemble model average. Changes in SST were evaluated using several different methods including estimating the linear trend in the SST time series from 1976 through 2099, both for annual and monthly means. The significance of the annual trends was evaluated using the Mann-Kendall test. We also examined changes in the mean and variability between periods, using 30-year intervals: 1976–2005 for the historical period and 2070–2099 for the future period. Variability in a given period was estimated from the standard deviation, and the change in variability is shown by the ratio between the variance in different periods, which provides the F-statistic. All values were computed for each model/simulation separately and then averaged together. The difference in means and variability between periods was assessed using two-sided t-tests and F-tests, respectively, computed for each model/simulation. The overall changes were deemed to be significant if 80% (50%) of the models showed a significant change in the t-test (F-test) at the 95% level (see Tebaldi et al., 2011). When comparing the variability and histograms between periods, we first detrended the SSTs in each period separately, because the mean trend could change over time and contribute to the apparent variability within a period.

The change in extremes through time was examined via the time series of SST anomaly in each decade from 1980–2100. The anomalies are relative to the monthly climatology from each individual climate model averaged over the period 1976–2005. The time of emergence, also referred to as climate departure, indicates when a future climate becomes "different" than the past. Here we used a very stringent measure for climate departures: when SSTs in the future exceed the *warmest* year or corresponding calendar month during the historical period. The percentage of years that exceeds this threshold based on the individual CMIP5 values reduces the potential for underestimating the uncertainty in the time of emergence (Hawkins et al., 2014).

Results

SST trends

The CMIP5 ensemble mean linear SST trend over the period 1976–2099 based on all calendar months is shown in **Figure 1a**. The trend is positive over most of the domain, which includes the eastern North Pacific,

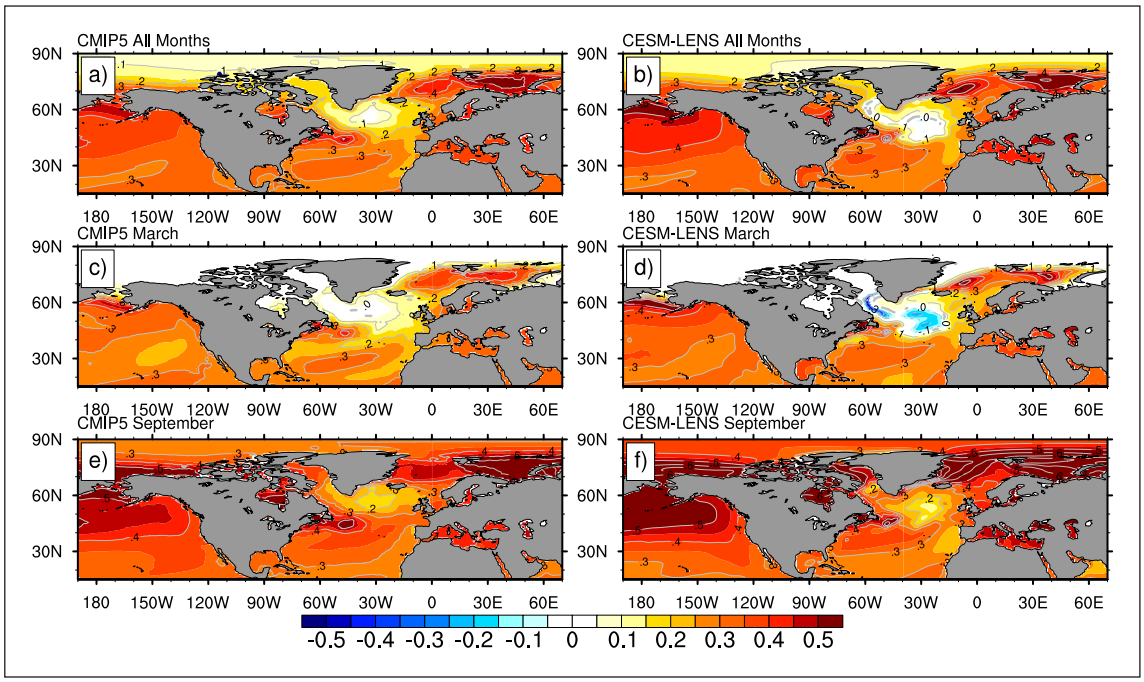

Figure 1: Ensemble mean SST trends from CMIP5 and CESM-LENS over the period 1976–2099. Trends are shown for all months **(a, b)**, for March **(c, d)** and for September **(e, f)** based on CMIP5 (a, c and e) and CESM-LENS (b, d), and f). Color bar indicates trends in °C decade^{-1} with positive (negative) values in shades of red (blue). Only trends that are significant at a 95% level using a Mann-Kendall test are shown. Trends are positive and significant in most areas except the North Atlantic and Arctic Oceans in March. DOI: https://doi.org/10.1525/elementa.191.f1

the North Atlantic and the Arctic oceans. It varies from approximately 0.25° to 0.5°C decade^{-1} with the strongest warming in the Bering Sea, along ~45°N in the western North Atlantic and in the Norwegian and Barents seas. The main exception occurs from the Labrador Sea to the southeast of Greenland, where there is little if any warming. The pattern and magnitude of the trends are very similar in the CESM-LENS ensemble mean including an absence of warming to the southeast of Greenland but with stronger warming in the Bering Sea and Greenland Sea (**Figure 1b**). The lack of warming south of Greenland results from a reduction in the poleward transport of warm water in the upper ocean by the Atlantic meridional overturning circulation (AMOC) and lengthened exposure to surface cooling as sinking at high latitudes decreases (Drijfhout et al., 2012; Cheng et al., 2013).

In general, the SST trends in March and September indicate that the warming is greater during summer than winter over most of the domain but especially at mid and high latitudes (**Figure 1c–f**). Indeed, the entire domain warms during September, but portions of the Labrador Sea and the northern North Atlantic exhibit a cooling trend during March in CESM-LENS (**Figure 1d**). The seasonal difference in the trend is also pronounced in the Arctic and surrounding seas. Most CMIP5 models project sea ice to decrease drastically during the 21st century in summer but still have thin ice cover over much of the Arctic during winter (supplemental Figures S1 and S2). The absence of ice allows for warming during summer, but ice restricts the SST to the freezing point of seawater (~–1.8°C), curtailing increases in SST during winter.

The annual linear SST trends during 1976–2099 in the 18 LME regions, obtained from the ensemble mean value of the CMIP5 models, are depicted in **Figure 2**. The annual trends are all positive, ranging from approximately 0.05 to 0.5°C decade^{-1}. A linear trend provides a good approximation of the overall SST changes in most LMEs (Climate Change Web Portal, 2017).

The monthly SST trends for 1976–2099 in CMIP5 and CESM-LENS are shown for the LMEs adjacent to North America (**Figure 3**) and for LMEs in the Arctic and European sectors (**Figure 4**). The median and even the 25th percentile of the trends in both sets of experiments are positive in all regions for all months. The spread exhibited by the models within CMIP5 is much larger than in CESM-LENS, suggesting that the disparity in trend estimates is mainly due to the differences between the models (e.g., resolution, numerical methods, parameterizations), rather than due to internal variability (within a single model). Despite the overall warming, the large spread in the CMIP5 estimates results in at least one model exhibiting cooling during at least one month in the Newfoundland-Labrador Shelf and Central Arctic regions, and in the Greenland, West Greenland, Iceland and Barents Seas. Negative trends are likely related to a particular model's reduction in AMOC in response to increasing greenhouse gases and to the areas in the North Atlantic where AMOC most strongly impacts SSTs as suggested by the findings of Cheng et al. (2013), Wang et al. (2014), and Céline (2017).

Consistent with **Figure 1**, the amplitude of the SST trend in most LMEs is greater during summer than in winter months (**Figures 3** and **4**), altering the seasonal cycle over the 21st century. The seasonal cycle of SSTs in

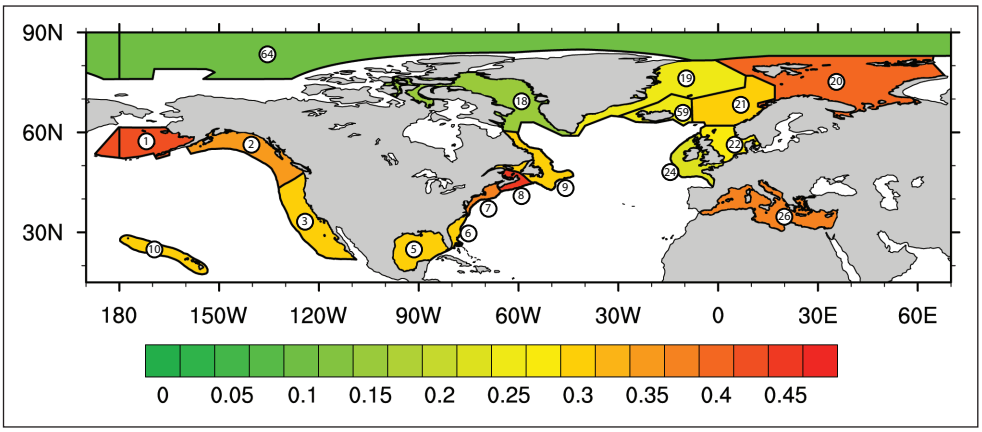

Figure 2: SST trends in Large Marine Ecosystems in the Arctic and around North America and Europe. Colors denote the CMIP5 ensemble mean area-averaged SST trends (°C decade^{-1}) during 1976–2099. All trends are significant at the 95% level using a Mann-Kendall test. Regions are numbered following the LME convention: 1) Bering Sea, 2) Gulf of Alaska, 3) California Current, 5) Gulf of Mexico, 6) Southeast US Shelf, 7) Northeast US Shelf, 8) Scotian Shelf, 9) Newfoundland-Labrador Shelf, 10) Hawaii, 18) West Greenland, 19) Greenland Sea, 20) Barents Sea, 21) Norwegian Sea, 22) North Sea, 24) Celtic-Biscay Shelf, 26) Mediterranean, 59) Iceland Shelf and Sea, and the 64) Central Arctic. DOI: https://doi.org/10.1525/elementa.191.f2

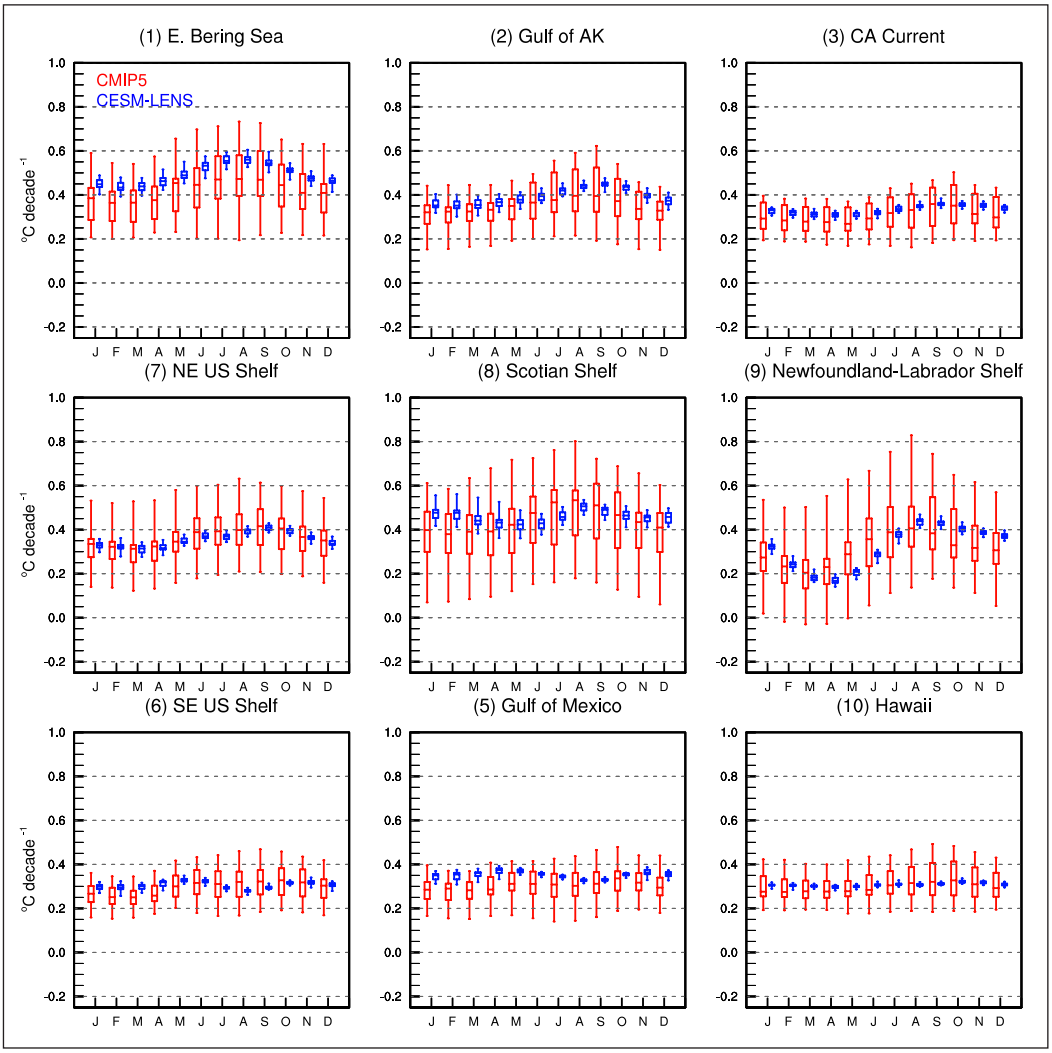

Figure 3: Monthly SST trends during the period 1976–2099 for LMEs around North America. SST Trends (°C decade^{-1}), computed for each model from the CMIP5 (red) and CESM-LENS (blue) experiments, are shown in box and whiskers format, where the end points indicate the maximum and minimum values, the box boundaries indicate the inter-quartile range (25% to 75%), and the median is the central line. The larger spread in CMIP5 relative to CESM-LENS indicates the range of trends is substantially greater among different models than due to internal variability in an individual model. DOI: https://doi.org/10.1525/elementa.191.f3

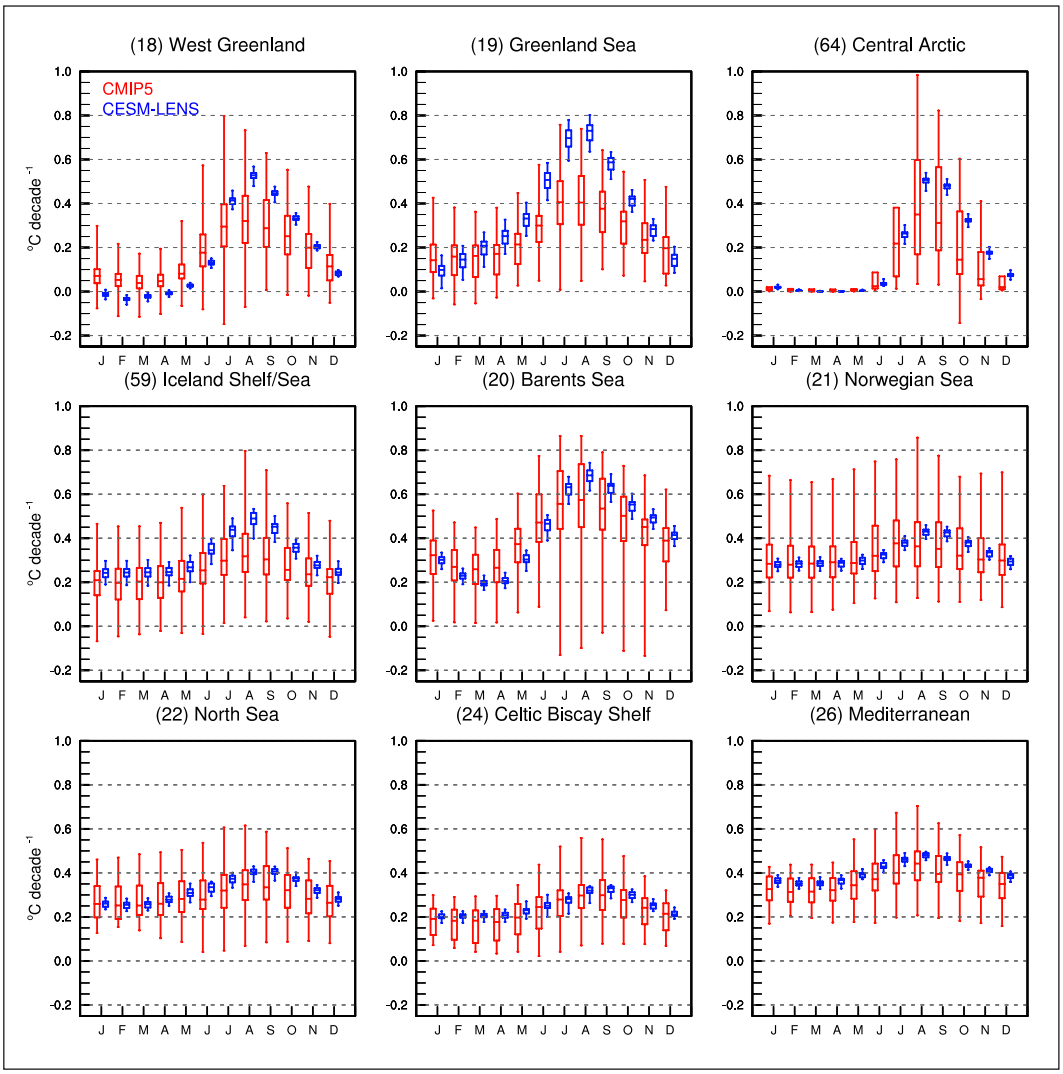

Figure 4: SST trends during the period 1976–2099 from LMEs in the Arctic and around Europe. SST Trends (°C decade^{-1}), computed for each model from the CMIP5 (red) and CESM-LENS (blue) experiments, are shown in box and whiskers format, where the end points indicate the maximum and minimum values, the box boundaries indicate the inter-quartile range (25% to 75%), and the median is the central line. The larger spread in CMIP5 relative to CESM-LENS indicates the range of trends is substantially greater among different models than due to internal variability in an individual model. DOI: https://doi.org/10.1525/elementa.191.f4

the 18 LMEs obtained from observations and the CMIP5 ensemble mean, averaged over the historical period, are shown in **Figures 5** and **6**. Values are presented for the calendar months after removing the annual mean. The simulated seasonal cycle is very close to observations in most regions, although its amplitude is underestimated in the Northeast US Shelf, Scotian Shelf and Barents Sea LMEs. The SST seasonal cycle for future periods, and the percent difference between the two periods, is also shown in **Figures 5** and **6**. The temperature differences with the mean included between the periods from the range of CMIP5 models are shown in Figures S3 and S4-. In nearly all regions, the CMIP5 SST departures relative to the annual mean are colder in winter and warmer in summer, amplifying the seasonal cycle in the future relative to the historical period. The main exceptions are in the Gulf of Mexico region, where there is a very slight lengthening of summer, and in the California Current and Hawaii LMEs, where the seasonal cycle shifts slightly later in the year. The percent change during winter and summer months ranges between 3% and 8% for most subtropical, mid-latitude and Pacific regions but exceeds 20% in many high latitude LMEs in the North Atlantic and European sectors. In addition to changes in sea ice (described above), the amplified seasonal cycle in the seas adjacent to the Arctic may result from the large mean seasonal cycle in MLD in these LMEs (discussed below).

Changes in warm extremes

In addition to the long-term warming trend, SST changes also manifest in shorter-term extremes. The largest monthly SST anomaly in each decade from the CMIP5, CESM-LENS and observations are shown in **Figures 7** and **8**. The anomalies, which can occur at any time of the year, are relative to the monthly climatology averaged over the period 1976–2005. There is a strong upward trend in the model simulations over the course of the 21st century, with a general increase in the CMIP5 model spread. For example, in the Bering Sea the median value of the decadal maximum as simulated by the CMIP5 models

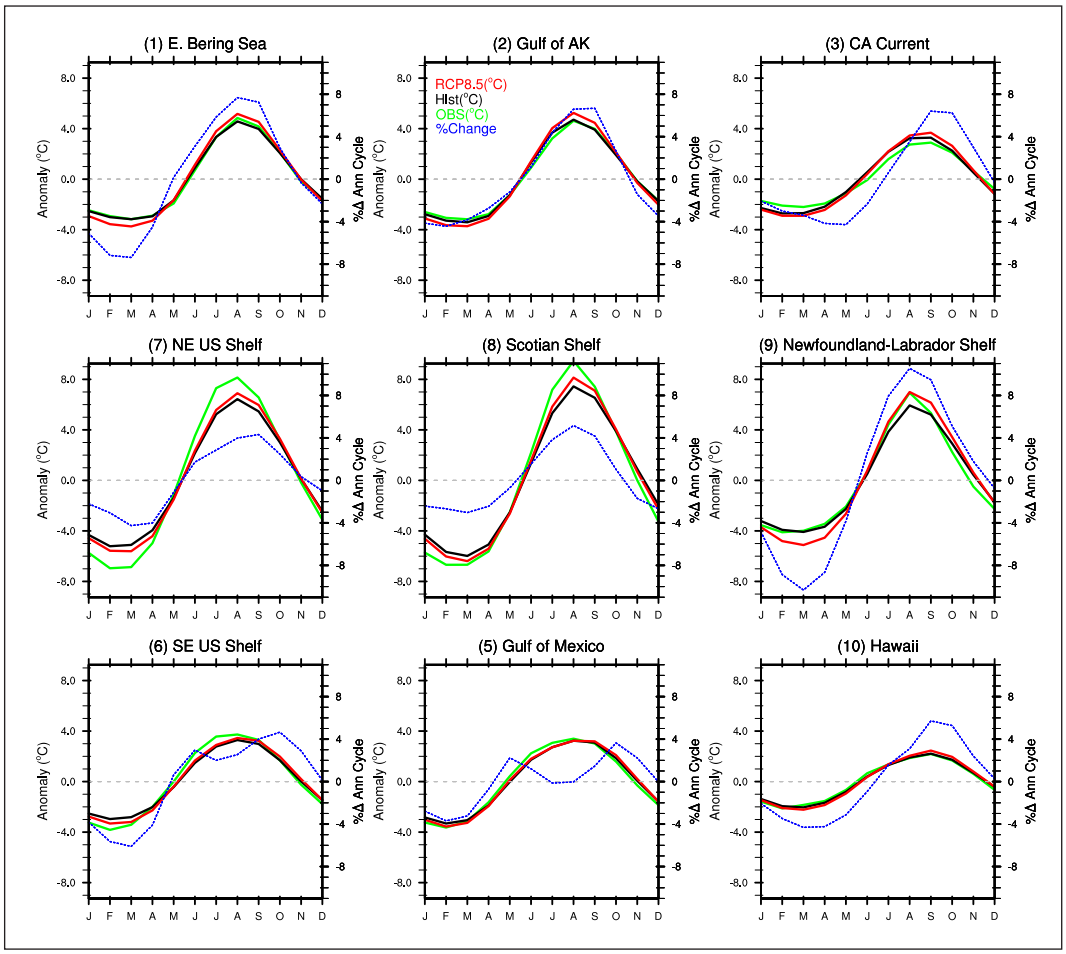

Figure 5: The mean seasonal cycle of SST (°C) for LMEs around North America. Hadley observations for the historical period (1976–2005) are in green, the CMIP5 ensemble mean during the historical period are in black, and the ensemble mean CMIP5 RCP8.5 experiments in the future period (2070–2099) are in red. Note the annual mean SST in each period has been subtracted. The percent change between the historical and future periods is shown in blue. The seasonal cycle is amplified in the future period. DOI: https://doi.org/10.1525/elementa.191.f5

increases from ~1.3°C in the 1980s to ~6.3°C in the 2090s, where the values range from approximately 0.5°–3.0°C in the 1980s to 3.5°–9.8°C in the 2090s. The spread is much smaller in the CESM-LENS set of simulations, indicating that the differences between the models, rather than internal variability (as estimated by the CESM-LENS), contribute most to the spread.

Given the large amount of internal climate variability and relatively modest signal for regional SST changes *during the historical period*, the observed decadal maximum (as one "realization" of nature) will not necessarily be close to the median model value even for skillful climate models. In addition, the accuracy of individual models will vary between regions. Thus, as a broad check, the observed trend should lie within the range of the model projections. The observations are generally within the model spread and show an upward trend in decadal maxima in most regions (**Figures 7** and **8**), but the observed maximum is above all model values in the central Arctic and exhibits little change over time in the Barents Sea region. There is a large amount of inter-decadal variability in the observations relative to the upward trend in several regions. These results suggest that the climate change signal for decadal maxima is relatively small over the past 35 years, but the models indicate that the signal relative to intrinsic variability should increase greatly as the 21st century progresses.

Changes in variability

Will sea surface temperatures become more variable in the future due to increasing greenhouse gases? We first address this question by mapping the SST standard deviation (σ) over the North Atlantic and eastern North Pacific during the historical (1976–2005) and future (2070–2099) periods in March and September for CMIP5 (**Figure 9**) and CESM-LENS (Figure S5). During both March and September in the historical period, σ is relatively high in the Bering Sea, along the west coast of North America, at about 40°N associated with the North Pacific Current, and in the vicinity of 35°N, 160°W, where ENSO teleconnections strongly influence the ocean. In the Atlantic, σ is large along the Gulf Stream/North Atlantic Current and along the northern rim of the basin from the Labrador Sea to the Barents Sea. Regions of high variability along the ice edge shift northward as the ice retreats from March to September. Comparing σ between the historical and future periods shows a clear enhancement in variability at higher latitudes (north of approxi-

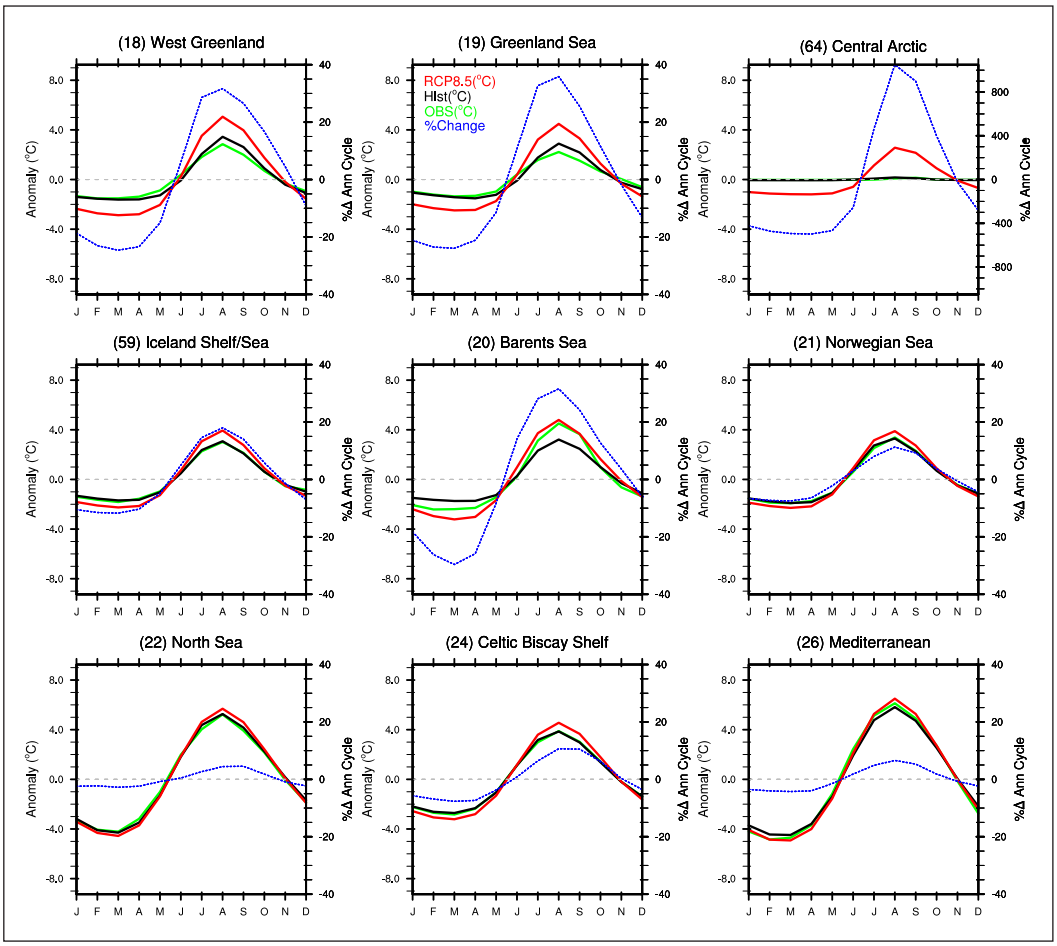

Figure 6: CMIP5 ensemble mean seasonal cycle of SST (°C) for LMEs in the Arctic and around Europe. Hadley observations for the historical period (1976–2005) are in green, the CMIP5 ensemble mean during the historical period are in black, and the ensemble mean CMIP5 RCP8.5 experiments in the future period (2070–2099) are in red. Note the annual mean SST in each period has been subtracted. The percent change between the historical and future periods is shown in blue. The seasonal cycle is amplified in the future period. DOI: https://doi.org/10.1525/elementa.191.f6

mately 60°N) in September (compare **Figure 9b** and **d**), where the disappearance of sea ice (Figure S1) allows for much larger fluctuations in SST. Changes in σ over the remainder of the domain in both winter and summer are subtle.

To highlight the differences between periods, the SST variance (σ^2) ratio in the future relative to the historical period in CMIP5 is also shown in **Figure 9**. The significant changes in SST variance (hatching) include increases in the Arctic in March as well as September. The percentage changes in March could be large in regions/models where ice disappears, even though the magnitudes of the changes are small (not shown). As SST σ^2 is high on the equatorward side of the ice edge where air-sea heat fluxes are strong and variable, the poleward retreat of the ice in the future (Figures S1 and S2) will result in a decrease in SST σ^2 in areas south of where the ice edge was located during the historical period. Thus, the poleward shift of the ice edge could explain the significant decrease in SST σ^2 in the southern Bering Sea, Labrador Sea and Barents Sea. The ratio of SST σ^2 increases significantly north of ~40°N over much of the eastern Atlantic but decreases south of Greenland in March. The changes in σ^2 are not significant over much of the remainder of the domain in March and nearly all of the North Atlantic and eastern Pacific in September. The variance changes are similar in the CESM-LENS with the exception of the Labrador Sea (Figure S5).

The ability of the CMIP5 models to simulate the observed distribution of SST anomalies in the LMEs was assessed by comparing the simulated and observed histograms shown in Figures S6 and S7. Overall, there is reasonably good agreement between the simulated and observed SST distribution, although in the Hawaii LME and the Bering, Greenland and Norwegian seas the simulated distribution is broader (less peaked) than observed, while the reverse is true for the California Current. However, the shift in the distribution due to climate change (**Figures 10** and **11**) is much larger than the difference between the observed and simulated histograms in all 18 regions.

How does the probability distribution of SST anomalies in the LMEs change due to both a shift in the mean as well as in the variability as the climate warms? To address this question, histograms of the monthly SST anomalies from the CMIP5 simulations during the historical (black line) and future (red line) periods are shown for the LMEs

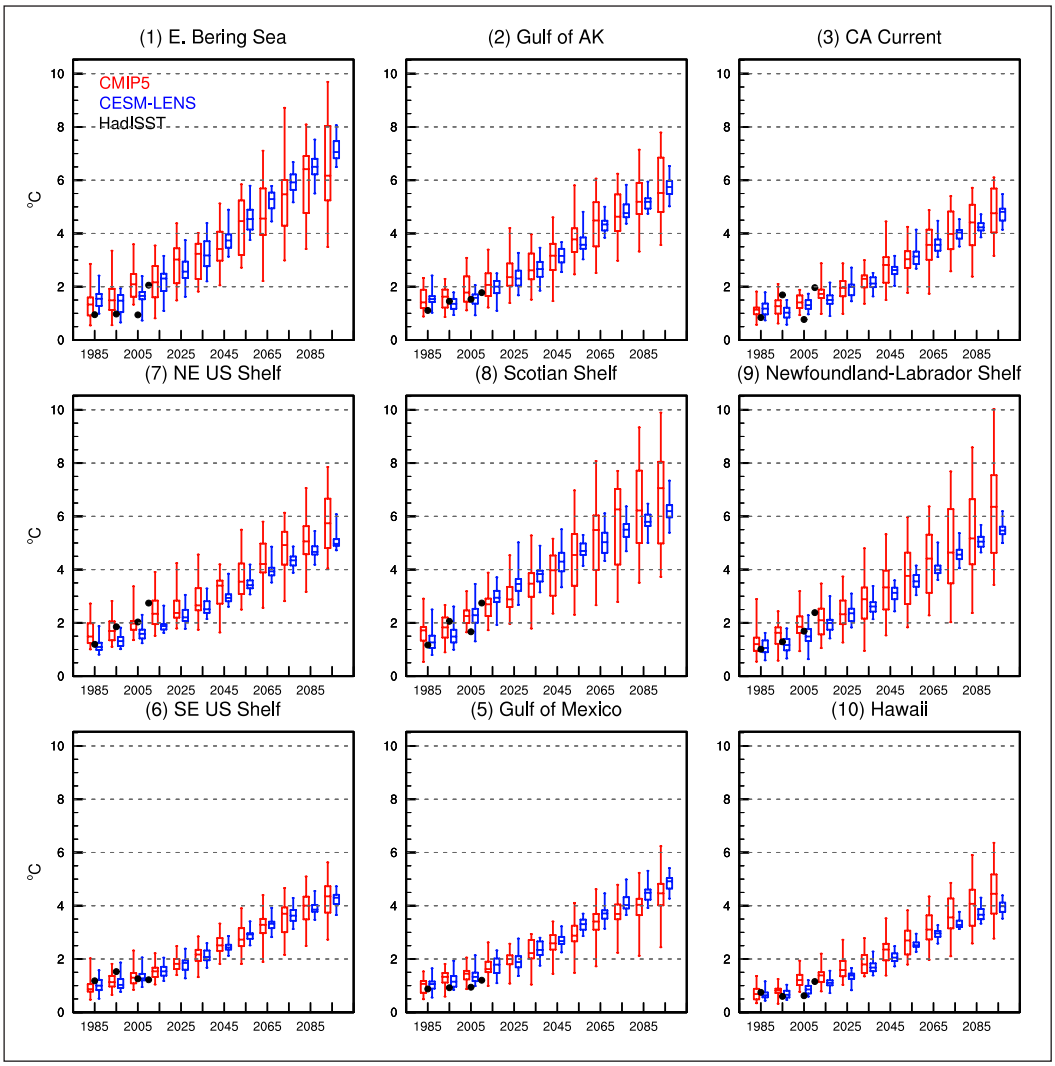

Figure 7: Maximum monthly SST anomalies per decade for LMEs around North America. The anomalies are relative to the historical period (1976–2005). They were obtained from the individual CMIP5 (red) and CESM-LENS (blue) simulations. They are shown in box and whiskers format, where the end points are the maximum and minimum values, the box boundaries are the inter-quartile range (25%–75%) and the median is the central line. Hadley SST observations are shown with black dots for the 1980s, 1990s, 2000s and the period 2006–2016. The observations lie within the range of the model variability for most LMEs. DOI: https://doi.org/10.1525/elementa.191.f7

in **Figures 10** and **11**. The trend has been removed from each 30-year period separately before computing the histograms, as it is generally larger in the future than in the historical period (**Table 1**). Curves for the future period are shown with (red solid line) and without (red dashed line) the mean difference between the periods included; the latter facilitates the comparison of the amplitude and shape of the distributions in the two periods. All regions show a substantial shift of the distribution to warmer values due to an increase in the mean. The shift is so large that for most LMEs all of the SSTs during the last 30 years of the 21st century will be greater than the mean in the historical period, i.e., even the coldest anomalies relative to the 1976–2005 climatology will be greater than zero (red solid curves in **Figures 10** and **11**). However, the change in the width or shape of the distributions is very small in most regions, including little change in the tails of the distributions. The minimal changes in the distributions are corroborated by similar σ values during the historical and future periods (**Table 1**). The largest changes occur in the central Arctic and Barents Sea LMEs, likely due to the elimination of sea ice enabling more SST variability (as discussed above). There is also a slight increase in SST variability for some eastern North Atlantic LMEs, including the Celtic Biscay Shelf.

Climate departures

A metric of the departure of future climates from the historical period, is given by the percentage of years in which the annual mean SSTs exceed the warmest year in the historical period (1976–2005). Maps of this metric, obtained from the CMIP5 models, are shown for three 30-year periods: 2010–2039, 2040–2069 and 2070–2099 in **Figure 12**. The percentage of years exceeding this threshold during 2010–2039 is fairly small, but still exceeds about half the years in the subtropical Atlantic, where internal variability is low. As the climate warms though the 21st century, a much larger fraction of years during 2040–2069 surpass the maximum value in the historical period, with exceedance rates of >80% over

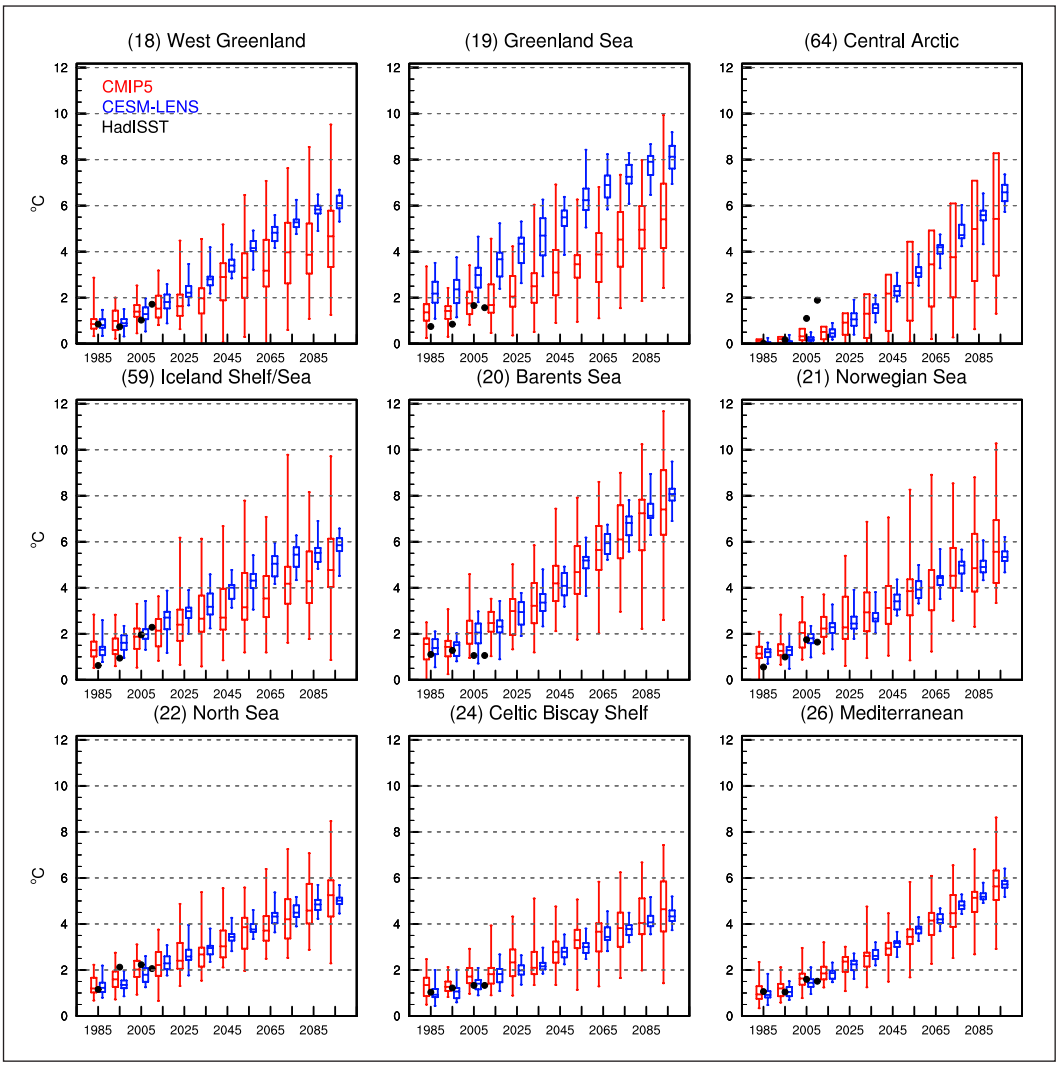

Figure 8: Maximum monthly SST anomalies per decade for LMEs in the Arctic and around Europe. The anomalies are relative to the historical period (1976–2005). They were obtained from the individual CMIP5 (red) and CESM-LENS (blue) simulations. They are shown in box and whiskers format, where the end points are the maximum and minimum values, the box boundaries are the inter-quartile range (25%–75%) and the median is the central line. Hadley SST observations are shown with black dots for the 1980s, 1990s, 2000s and the period 2006–2016. The observations lie within the range of the model variability for most LMEs. DOI: https://doi.org/10.1525/elementa.191.f8

much of the subtropical, midlatitude and Arctic oceans. By 2070–2090 more than 95% of the years exceed the warmest year in the late 20th century over nearly all of the domain except for the northern North Atlantic, where the climate change signal is small or absent and intrinsic variability is large.

The percentage of months in each decade of the 21st century in which SSTs exceed the warmest value during the corresponding calendar month in the historical period is shown for the 18 LMEs in **Figures 13** and **14**. The fraction of months exceeding this threshold increases over all decades in the 21st century in all regions, but the rate of change and the spread among CMIP5 models varies greatly between regions. For example, in the Gulf of Mexico the percentage exceeding the maximum value in the historical period during 2040–2050 (indicated by the values at 2040) has a median value of ~75% (red line) and ranges from approximately 50% to 100% (lightest gray), while in the Greenland Sea, the median values are lower (~35%) and the uncertainty larger (range of 0%–100%). The time series of the annual anomalies relative to the maximum annual SST value during 1976–2005 indicates that the median CMIP5 value exceeds the historical value in all 18 LMEs by ~2050 (Figures S8 and S9).

The observed exceedance values (black line) during 10-year periods from 1980 are also presented in **Figure 13** and **14**. The observed values exhibit an upward trend in all 18 regions and generally lie within the model spread (also see Figures S8 and S9). However, the observed values of ~18% and 35% are at the very upper end of the model range in the West Greenland and Scotian Shelf LMEs, during 2005–2015, the last period with observations.

MLD and its influence on SST

The average mixed layer depth north of 20°N in March and September for the historical and future periods as well as the difference between them obtained from CMIP5 and the CESM-LENS ensemble means are shown in **Figure 15**. During the historical period, the MLD is greater than 50 m over most of the North Atlantic and eastern North Pacific

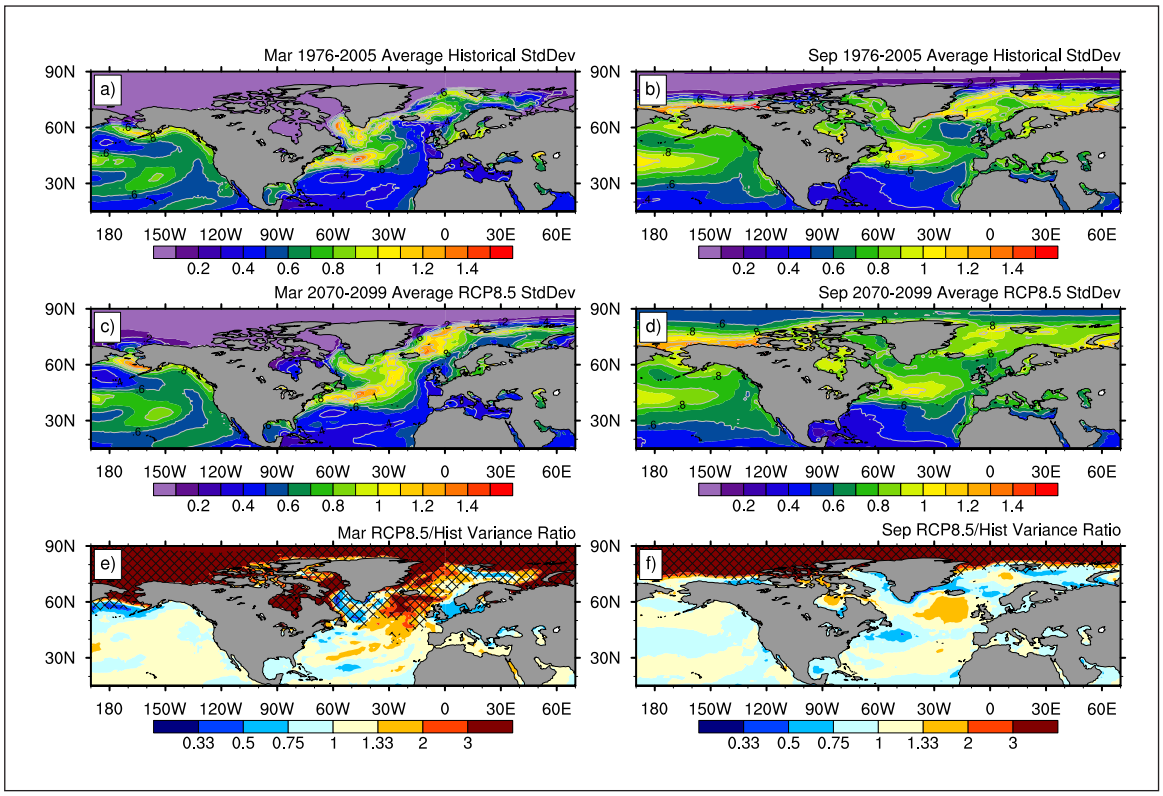

Figure 9: CMIP5 ensemble mean interannual SST standard deviation (°C). The year-to-year SST standard deviation (σ) for the historical period 1976–2005 **(a, b)** and the future period 2070–2099 **(c, d)**, along with the future/historical SST variance (σ^2) ratios **(e, f)**, for both March (a, c, e) and September (b, d, f). The SST anomalies are computed for each model separately, de-trended within their respective periods, and the standard deviation (and the variance) are computed for each individual model and then averaged together. The variance ratios are cross-hatched, where >50% of the models show a significant change at the 95% level. Significant changes in SST variance are mainly found at higher latitudes and in the northern north Atlantic in winter. DOI: https://doi.org/10.1525/elementa.191.f9

in March. It is substantially deeper (>100 m) between 30°N and 45°N in the North Atlantic and portions of the eastern North Pacific and exceeds 400 m in the Subarctic portion of the North Atlantic. The MLD is much shallower and more uniform in September when the range is 20–60 m. In general, MLDs are deeper in the CMIP5 then in CESM-LENS in winter, while the reverse is true during summer in the historical period. Recall that different methodologies were used to estimate MLD in CMIP5 and CESM-LENS due to how the data were archived.

In CMIP5 and CESM-LENS the MLD exhibits significant decreases in the future relative to the historical period over much of the domain in both March and September. The mixed layer shoals in the southern Labrador Sea and over much of the northern North Atlantic, shoaling by more than 100 m in March and 5 m in September in both data sets. Given the shallow climatological MLDs in summer, a 5–10 m change represents a substantial percentage change in the overall depth. The MLD also shoals over portions of the eastern Pacific and Atlantic north of ~30°N. The shallowing of the mixed layer likely results from enhanced stability as the heating from greenhouse gases is concentrated near the surface, with a decrease in salinity also contributing to increased stratification in the Arctic Ocean and northern portions of the Atlantic and the Pacific (Capotondi et al., 2012; Climate Change Web Portal, 2017). There are regions where the MLD increases, including approximately 70°N–80°N, likely due to the retreat of sea ice exposing these areas to wind mixing. The MLD also deepens in the subtropical eastern Atlantic in September, especially in CESM-LENS, due in part to an increase in the surface salinity, which makes the surface layer more convectively active. During March, the mixed layer also deepens in portions of the eastern North Atlantic, in both sets of model experiments, and in the Norwegian Sea in the CESM-LENS. The causes for this deepening are uncertain, but may be related to changes in surface wind stress (Capotondi et al., 2012) or advection of warm water at depth. While the magnitude of the MLD changes is generally larger in winter than in summer, the seasonal cycle of the LME MLD trends can vary considerably over the seasonal cycle (Figures S10 and S11). For example, in the Norwegian Sea the MLD shoals over time in November and December but deepens during February through May in CESM LENS (Figure S11).

Seasonal variability in addition to long-term changes in MLD can affect the SST response to increasing greenhouse gases, as heating from the atmosphere will be rapidly mixed over the surface layer of the ocean. The seasonal cycle of the SST trend relative to the monthly mean MLD during 1976–2005 obtained from CMIP5 and CESM-LENS is shown for the high latitude, midlatitude and subtropical regions in **Figure 16**. While the MLDs

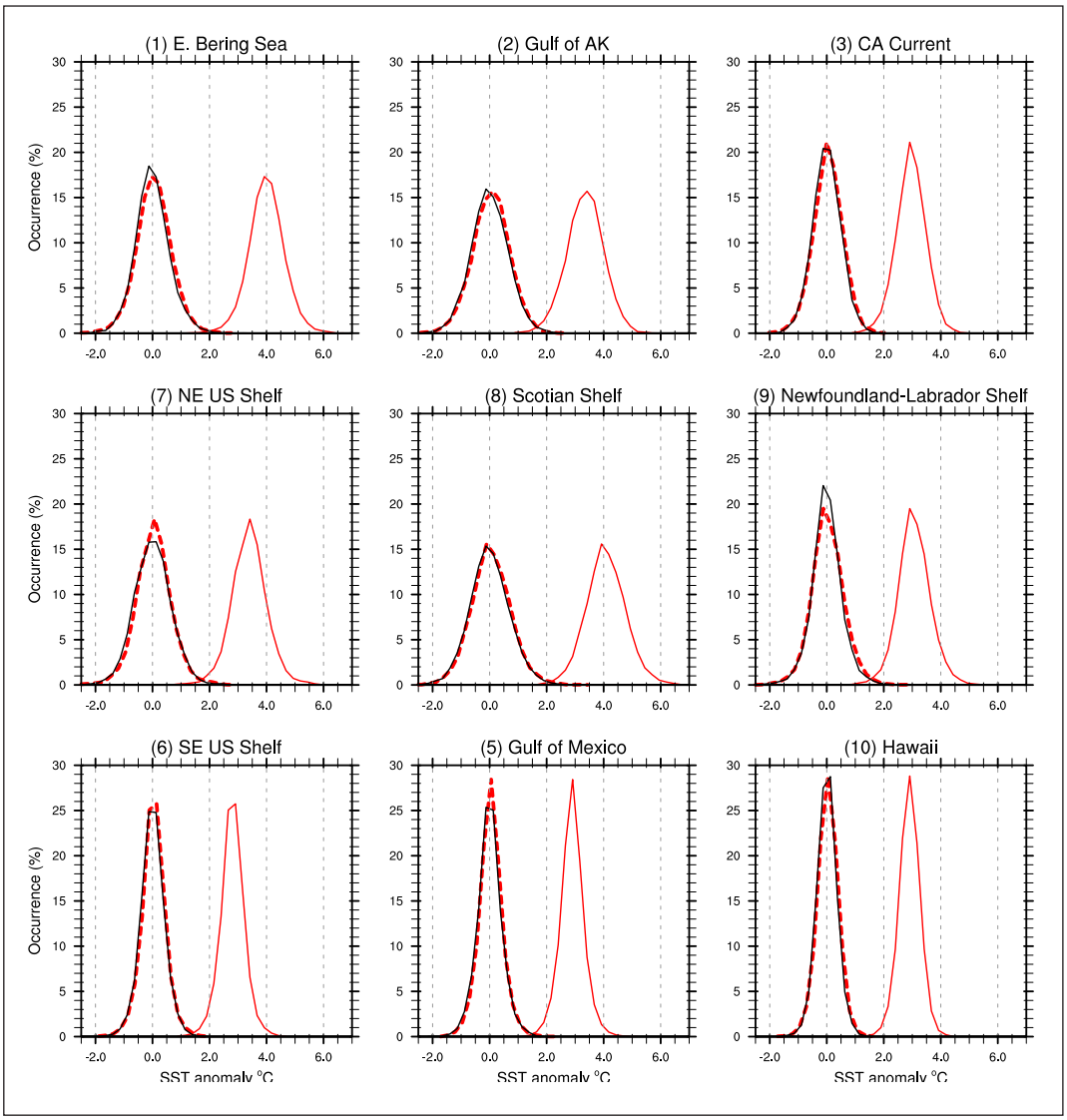

Figure 10: Probability distributions of CMIP5 monthly SST anomalies averaged over the LMEs around North America. The results are shown for the historical period (1976–2005, black lines) and future period (2070–2099, red lines), where the SSTs have been linearly detrended within each period. The red dashed line shows the future distribution of anomalies without the mean change to make it easier to compare the shapes of the future and historical distributions. Other than the change in the mean, the changes in the distributions are very small for most regions. DOI: https://doi.org/10.1525/elementa.191.f10

differ between the two sets of model experiments, several robust features emerge: *i*) the MLD is generally deepest during February or March and shallowest during June through August; *ii)* for nearly all regions, the SST trend decreases as the monthly mean MLD increases, and *iii*) because the MLD reaches a minimum of approximately 15–30 m in summer in all regions the seasonal range is primarily set by the deep MLDs in late winter, although the MLD may reach the ocean bottom at some LME gridpoints especially during winter. While the LMEs exhibit a wide seasonal MLD variability, the areas with the greatest range occur at mid and high latitudes. Thus, the mean seasonal cycle in MLD acts to increase the upward SST trend in summer relative to winter, amplifying the seasonal cycle of SST in the future, particularly at mid and high latitudes.

In several LMEs, the seasonal evolution of the relationship between SST trends and MLD exhibits an oval shape (**Figure 16**), which is indicative of a "hysteresis loop" whereby the current state of the system depends on its evolution through previous states. For example, in the Celtic Biscay Shelf LME (red curve middle panels), the temperature trend is lower in May to July (months 5–7) than from August to October (months 8–10) for similar MLDs. The hysteresis loop in the SST trend found here is similar to the evolution of seasonal mean SSTs (Gil and Turner, 1976) in that both are greater in fall than in spring for the same MLD. An SST-MLD hysteresis loop tends to occur due to the asymmetric ocean response to the surface heating and wind forcing over the seasonal cycle: the mixed layer reforms closer to the surface in spring, with no flux through the base of the mixed layer, but entrains water from below into the mixed layer when it deepens in fall into winter (Gill and Turner, 1976; Alexander et al., 2000). As a result, heat accumulates while the mixed layer remains shallow from late spring into early fall, which

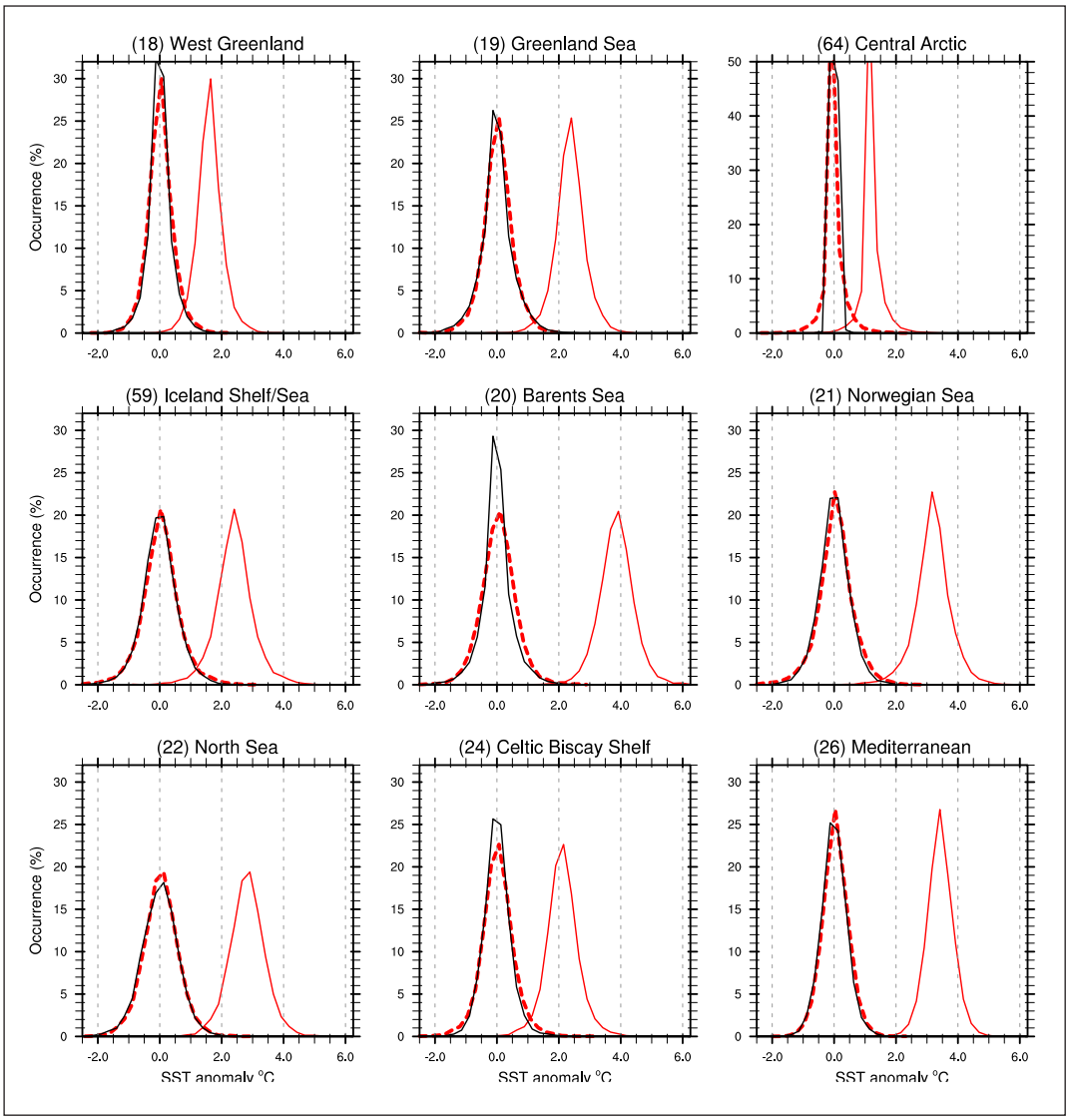

Figure 11: Probability distributions of CMIP5 monthly SST anomalies averaged over the LMEs in the Arctic around Europe. The results are shown for the historical period (1976–2005, black lines) and future period (2070–2099, red lines), where the SSTs have been linearly detrended within each period. The red dashed line shows the future distribution of anomalies without the mean change to make it easier to compare the shapes of the future and historical distributions. Other than the change in the mean, the changes in the distributions are very small for most regions. DOI: https://doi.org/10.1525/elementa.191.f11

contributes to the maximum SST trends occurring in August–September as opposed to June–July.

Summary and discussion

We examined changes in SSTs from 1976 to 2099 using one simulation from 26 models in the CMIP5 archive and 30 simulations of the NCAR CESM as part of the large ensemble project. All of the simulations use the observed forcings through 2005 and the RCP8.5 "business as usual" scenario for greenhouse gases through the remainder of the 21st century. Both sets of models show strong warming over the 21st century over most of the global oceans including the large marine ecosystems around North America, Europe, and the Arctic Ocean. The spread in the CMIP5 SST trends is generally larger than in the CESM-LENS, which indicates that there is greater uncertainty in the response to greenhouse gas forcing due to model differences (e.g., parameterizations, resolution, etc.) than internal climate variability. However, for some variables, such as regional sea level pressure changes in the extratropics, internal variability can be larger than the mean climate change signal (Deser et al., 2012b, 2014)

The projected warming trends are generally larger in summer than in winter. The enhanced warming in summer is consistent with previous regional studies (Chollett et al., 2012; López García and Belmonte, 2011; Shaltout and Omested, 2014) and with the enhanced amplitude of the observed seasonal cycle of SSTs in the northwest Atlantic (Friedland and Hare, 2007; Thomas et al., 2017). The summertime warming is especially pronounced at high latitudes, as portions of the Arctic Ocean and adjacent seas become ice free in summer, but it is still cold enough for a thin ice layer to reform in winter, enabling SSTs to increase well above freezing in summer but not in winter. Greater warming in summer may thermally

Table 1: CMIP5 SST trends (°C decade^{-1}) and inter-annual standard deviations (°C) with (w) and without (w/o) the trends for the historical (1976–2005, "20th C") and future (2070–2099, "21st C") periods in the 18 LME regions examined in this study. The NOAA-designated LME region numbers are also shown in the first column. DOI: https://doi.org/10.1525/elementa.191.t1

Large Marine Ecosystem	SST Trend: (°C Decade^{-1})		Std Dev (σ) w/Trend		Std Dev (σ) w/o Trend	
	20th C	21st C	20th C	21st C	20th C	21st C
(1) E. Bering Sea	0.25	0.54	0.68	0.82	0.59	0.61
(2) Gulf of AK	0.17	0.41	0.70	0.77	0.64	0.64
(3) CA Current	0.14	0.36	0.53	0.62	0.49	0.51
(5) Gulf of Mexico	0.18	0.37	0.47	0.54	0.43	0.41
(6) SE US Shelf	0.18	0.35	0.46	0.53	0.41	0.42
(7) NE US Shelf	0.22	0.42	0.71	0.76	0.64	0.63
(8) Scotian Shelf	0.26	0.54	0.77	0.87	0.69	0.70
(9) Newfoundland-Labrador Shelf	0.19	0.49	0.59	0.74	0.53	0.57
(10) Hawaii	0.16	0.39	0.40	0.52	0.34	0.36
(18) West Greenland	0.08	0.27	0.42	0.53	0.38	0.41
(19) Greenland Sea	0.09	0.33	0.57	0.66	0.52	0.47
(20) Barents Sea	0.14	0.50	0.56	0.79	0.49	0.56
(21) Norwegian Sea	0.19	0.36	0.61	0.75	0.50	0.58
(22) North Sea	0.22	0.31	0.66	0.68	0.59	0.57
(24) Celtic Biscay Shelf	0.19	0.26	0.50	0.62	0.43	0.53
(26) Mediterranean	0.23	0.45	0.48	0.59	0.41	0.42
(59) Iceland Shelf/Sea	0.09	0.32	0.65	0.78	0.57	0.62
(64) Central Arctic	0.14	0.32	0.06	0.56	0.05	0.31

stress some marine organisms, while larger differences between summer and winter temperatures could modify the regional productivity, distribution and abundance of species (Edwards and Richardson, 2004).

The stronger SST trends in summer than in winter are partly due to the climatological seasonal cycle in MLD: shallow summer mixed layers allow heating from the atmosphere to be concentrated in a thinner ocean layer compared to winter. This effect is amplified where the summer-winter MLD differences are large, particularly in the Arctic Ocean and surrounding seas. In addition to the mean MLD seasonal cycle, SST trends and variability are also influenced by the greenhouse gas-induced changes in the MLD. The MLD decreases significantly over most of the North Atlantic and eastern North Pacific in both March and September due to an increase in near surface warming that enhances static stability (Capotondi et al., 2012; Climate Change Web Portal, 2017) and inhibits mixing. A decrease in MLD provides a positive feedback to SST increases over most of the oceans, because heating from the atmosphere due to increasing greenhouse gases is concentrated over a thinner ocean layer. SST trends are also influenced by changes in sea ice and dynamical ocean processes, including changes in ocean currents, upwelling and the strength and depth of the thermocline.

The SST distribution can change due to both a shift in the mean, a change in the amplitude of the variability or to a change in the type of distribution. These changes can all impact extreme values. The SST changes by the end of the 21st century are primarily due to a positive shift in the mean, such that there will be a large increase in warm extremes and decrease in cold extremes relative to the historical period (1976–2005), as exemplified in **Figures 10** and **11**. The shift in the mean was so large in many regions that SSTs during the last 30 years of the 21st century will *always* be warmer than the warmest year in the historical period. The "time of emergence", when the future (through the 21st century) stays warmer than at any time during the historical period, occurs much earlier at lower latitudes, consistent with the findings of Diffenbaugh and Scherer (2011) and Mora et al. (2013), due to the limited interannual variability relative to the climate change signal. Thus, mid and high latitude species that are acclimated to a wide temperature range may be better able to adjust to climate change than species in the Caribbean and low latitudes in general, even though the amplitude of the changes are larger at high latitudes.

With the mean shift and linear trend removed, the changes in probability distributions are generally small; i.e., the standard deviation and histograms of SST anomalies in

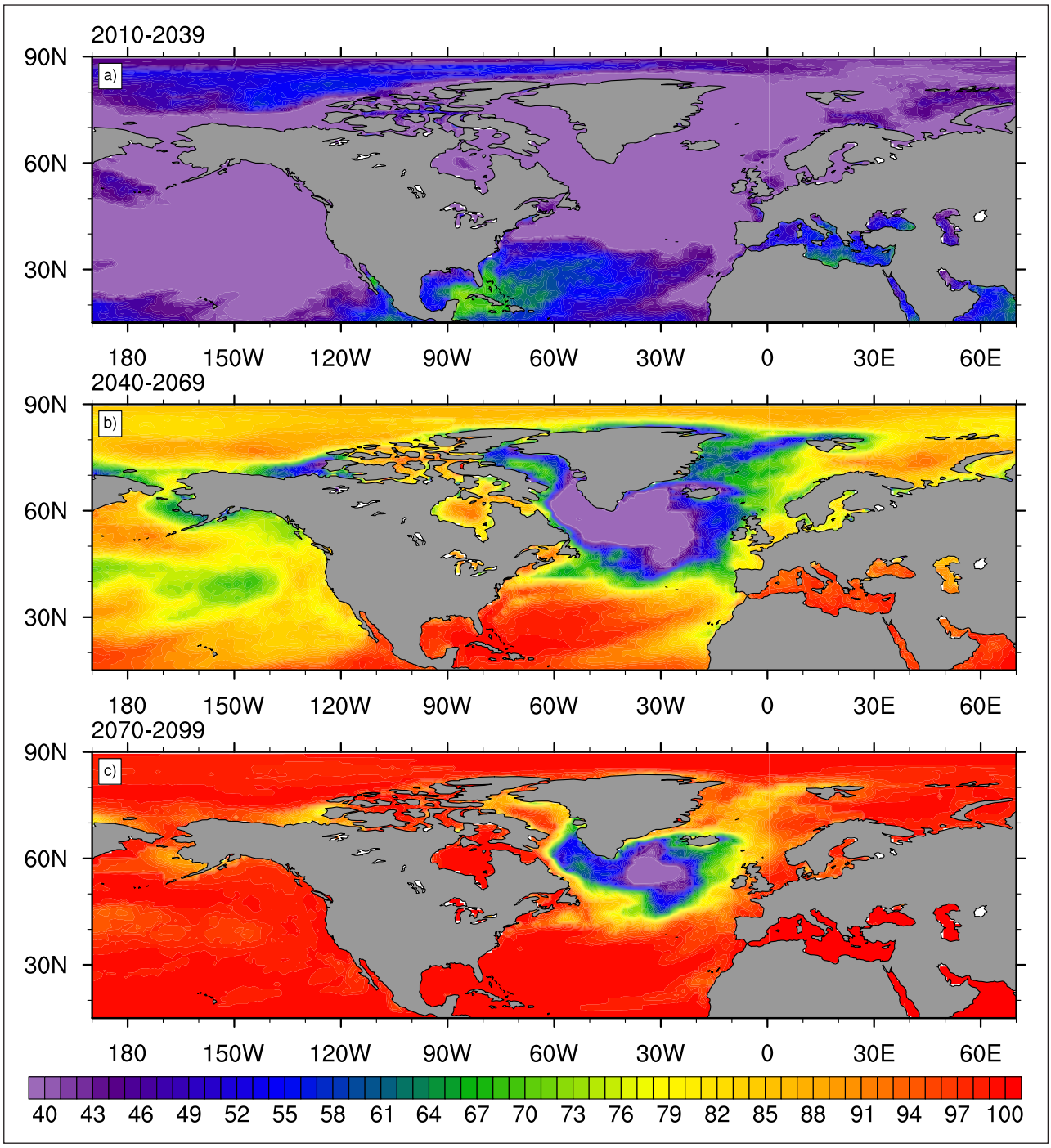

Figure 12: Percent of years with annual SST anomalies exceeding the maximum during the historical period (1976–2005). Shown are three different 30-year periods: **a)** 2010–2039, **b)** 2040–2069, **c)** 2070–2099. Percentages are computed for each CMIP5 model and then averaged together. Most of the northern oceans exceed the warmest historical year in the last three decades of the 21st century. DOI: https://doi.org/10.1525/elementa.191.f12

the LMEs were similar in the historical and future periods. Some regions, did exhibit an increase in the SST variability, including the Arctic Ocean and surrounding seas where the increase in ice-free periods allowed the water temperature to fluctuate, because it was not constrained to be at the freezing point. SST anomalies also exhibited enhanced variability in the future during March in the vicinity of Iceland. The reason for this increase is unclear but could be due to several factors including changes in the MLD, the North Atlantic Oscillation, storm track location and strength, and variability of the ocean gyres and AMOC.

The projected transition to much warmer conditions by the end of this century will likely have profound implications for marine ecosystems. At the end of the 21st century, temperatures in the Gulf of Maine could transition to be more like those near the New York Bight today, SSTs along

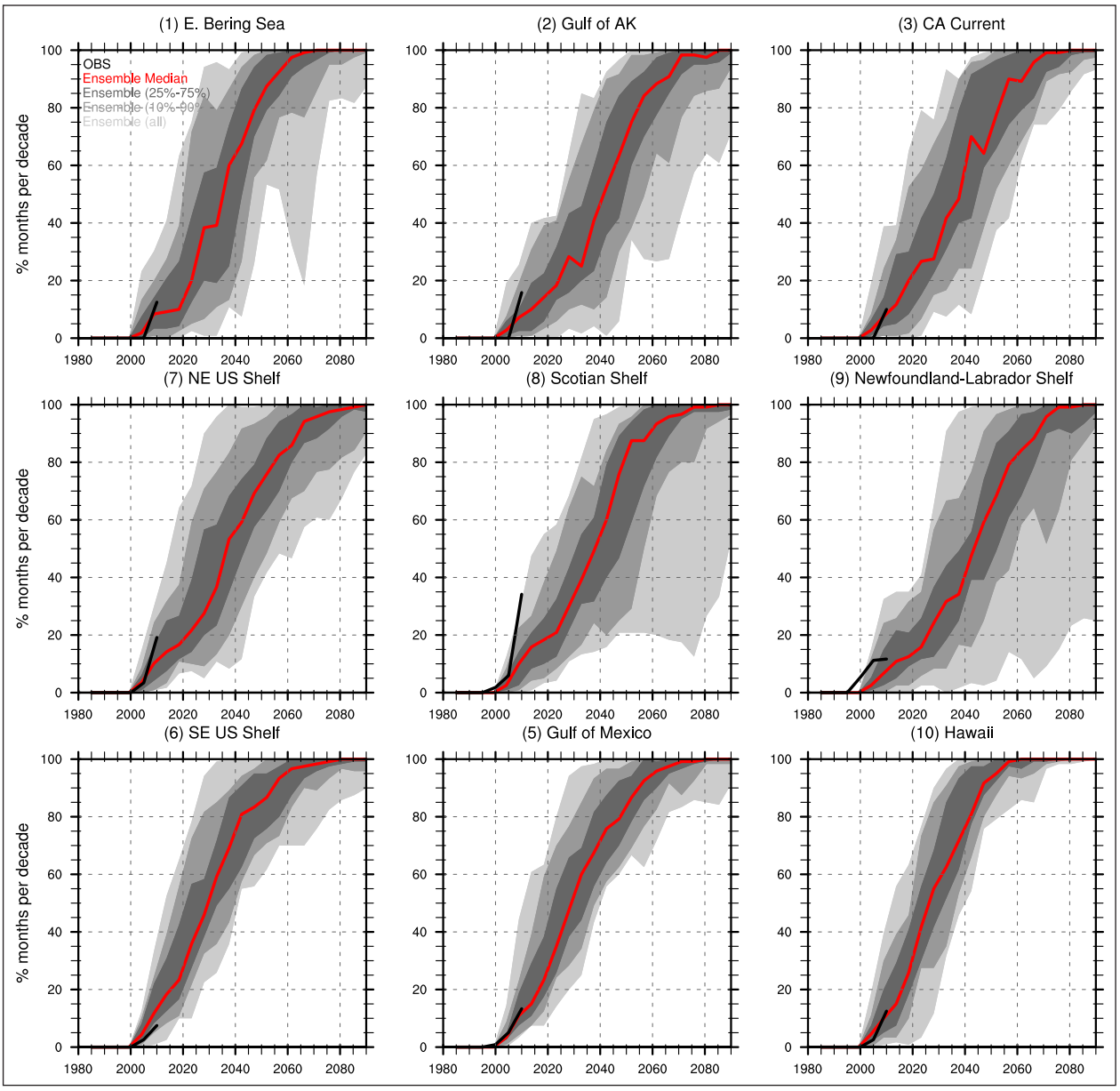

Figure 13: Percent of monthly SST anomalies in each decade that exceed the monthly maximum during 1976–2005. Results are shown for CMIP5 models in the LMEs around North America. The ensemble median is red and Hadley SST observations are black. The outer envelope (light gray) shows the ensemble max/min range. The 2nd envelope (medium gray) shows the 10th–90th percentile range of the ensemble and the inner envelope (dark gray) indicates the inter-quartile range (25th–75th percentile). The decades were sampled every five years in overlapping 10-year periods for smoothness. By mid-century most regions exceed the maximum during the historical period (1976–2005) more than 80% of the time. DOI: https://doi.org/10.1525/elementa.191.f13

the US west coast near the Canadian border could be more like those near central California, while SSTs in the northern Norwegian Sea could be more like current conditions east of England. The warming could result in poleward migration of some fish species, which has already been documented in North American and European marine ecosystems (Perry et al., 2005; Nye et al., 2009; Pinsky et al., 2013), and lead to profound changes in the structure of marine ecosystems that could necessitate a reevaluation of LME boundaries. The shift in the SST distribution results in exceptionally large warm extremes and the disappearance of cold extremes relative to the end of the 20th century in the RCP8.5 simulations. As the growth and reproduction of many species depends on their thermal tolerances, extreme temperatures could have a substantial impact on fish population dynamics and biodiversity (Pörtner et al., 2001; Pörtner and Peck, 2010; Lynch et al., 2014; Deutsch et al., 2015).

We have used RCP 8.5 simulations to examine changes in monthly SST anomalies with a focus on coastal regions

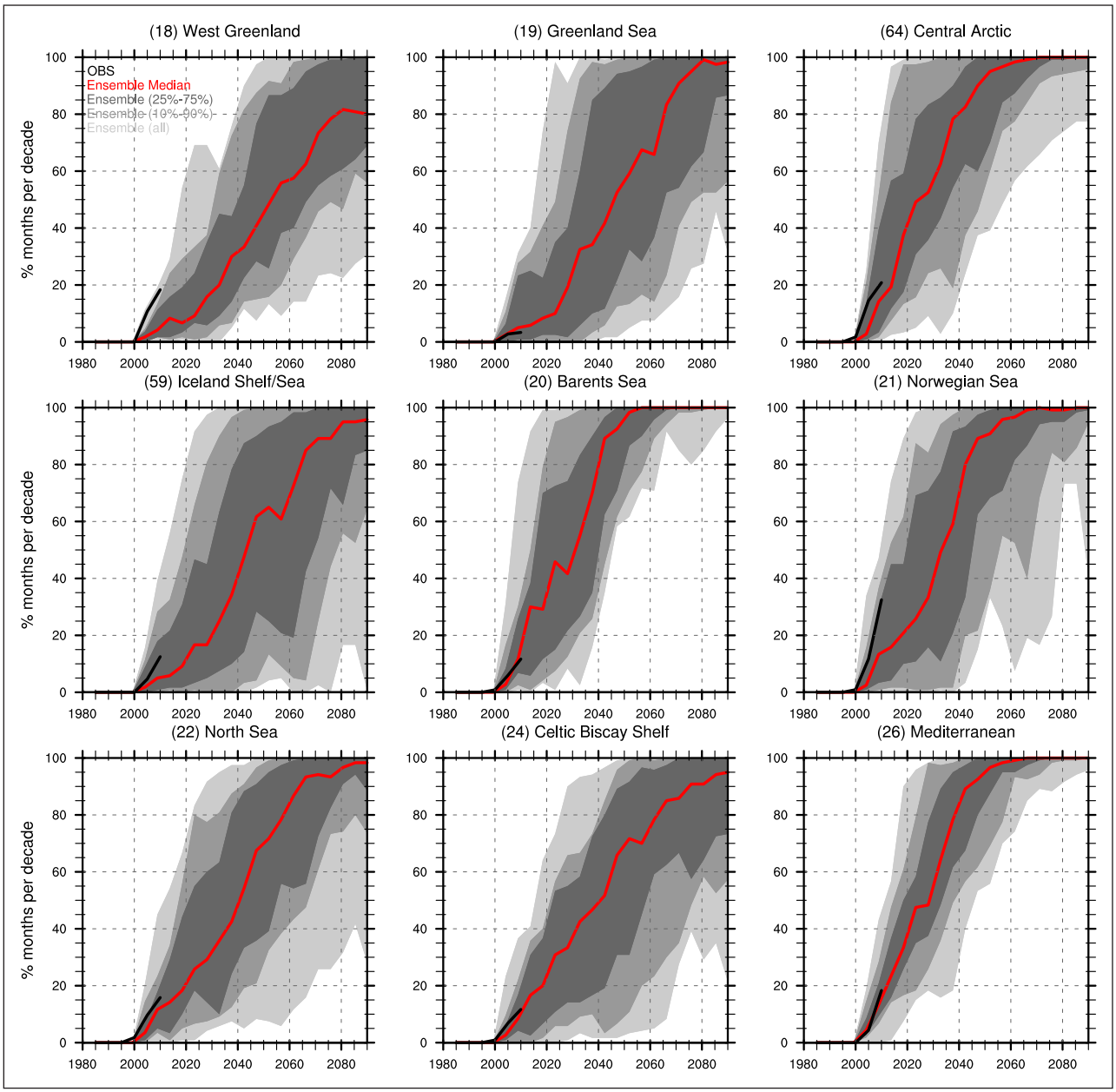

Figure 14: Percent of monthly SST anomalies in each decade that exceed the monthly maximum during 1976–2005. Results are shown for CMIP5 models in the LMEs in the Arctic and around Europe. The ensemble median is red and Hadley SST observations are black. The outer envelope (light gray) shows the ensemble max/min range. The 2nd envelope (medium gray) shows the 10th–90th percentile range of the ensemble and the inner envelope (dark gray) indicates the inter-quartile range (25th–75th percentile). The decades were sampled every five years in overlapping 10-year periods for smoothness. By mid-century most regions exceed the maximum during the historical period (1976–2005) more than 80% of the time. DOI: https://doi.org/10.1525/elementa.191.f14

in northern portions of the Pacific and Atlantic and in the Arctic Ocean. At ~1° horizontal resolution, the CMIP5 models do not adequately resolve many processes including ocean eddies, coastal upwelling, and interactions with topographic features, and where western boundary currents separate from the coast. While a few studies have used higher resolution models to assess the effects of climate change on SSTs (e.g., Chamberlain et al., 2012 and Saba et al., 2016), they have focused on a small region or are based on a single model run with idealized forcing. A broader assessment of climate change on a wide array of ocean variables, using additional forcing scenarios and higher resolution models, and at daily time scales are all warranted.

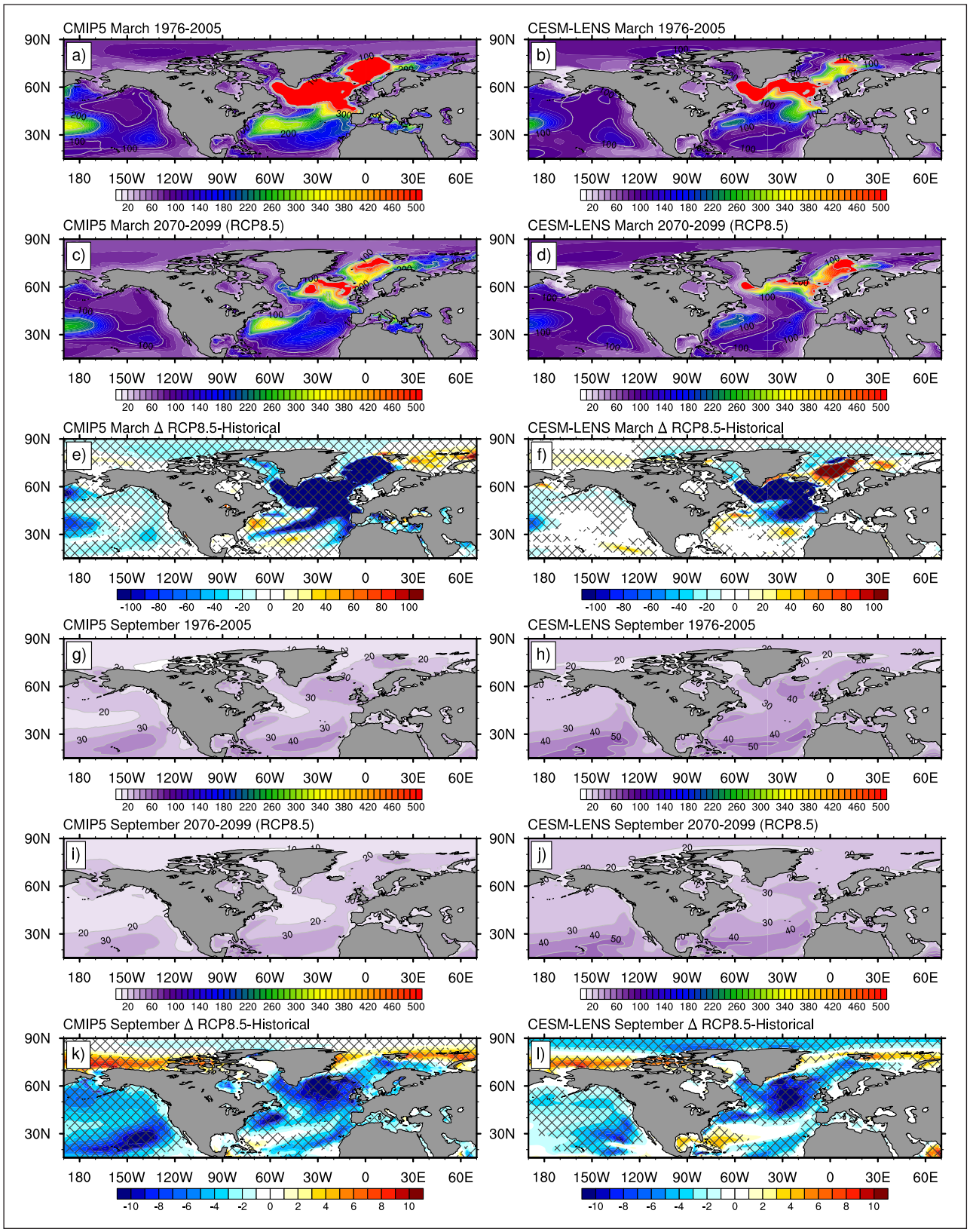

Figure 15: CMIP5 and CESM-LENS ensemble mean mixed layer depths (MLDs) during 1976–2005 and 2070–2099. The CMIP5 values are presented on the left and the CESM-LENS values on the right. Shown are the time averaged March MLDs (m) during 1976–2005 **(a, b)** and 2070–2099 **(c, d)**. The difference in March MLDs between the future (2070–2099) and historical (1976–2005) periods are shown in **(e** and **f)**. A similar set of maps but for September are presented in panels **(g–l)**. Changes in the MLD are cross-hatched where >80% of the models indicate a significant change based on a t-test at the 95% significance level. DOI: https://doi.org/10.1525/elementa.191.f15

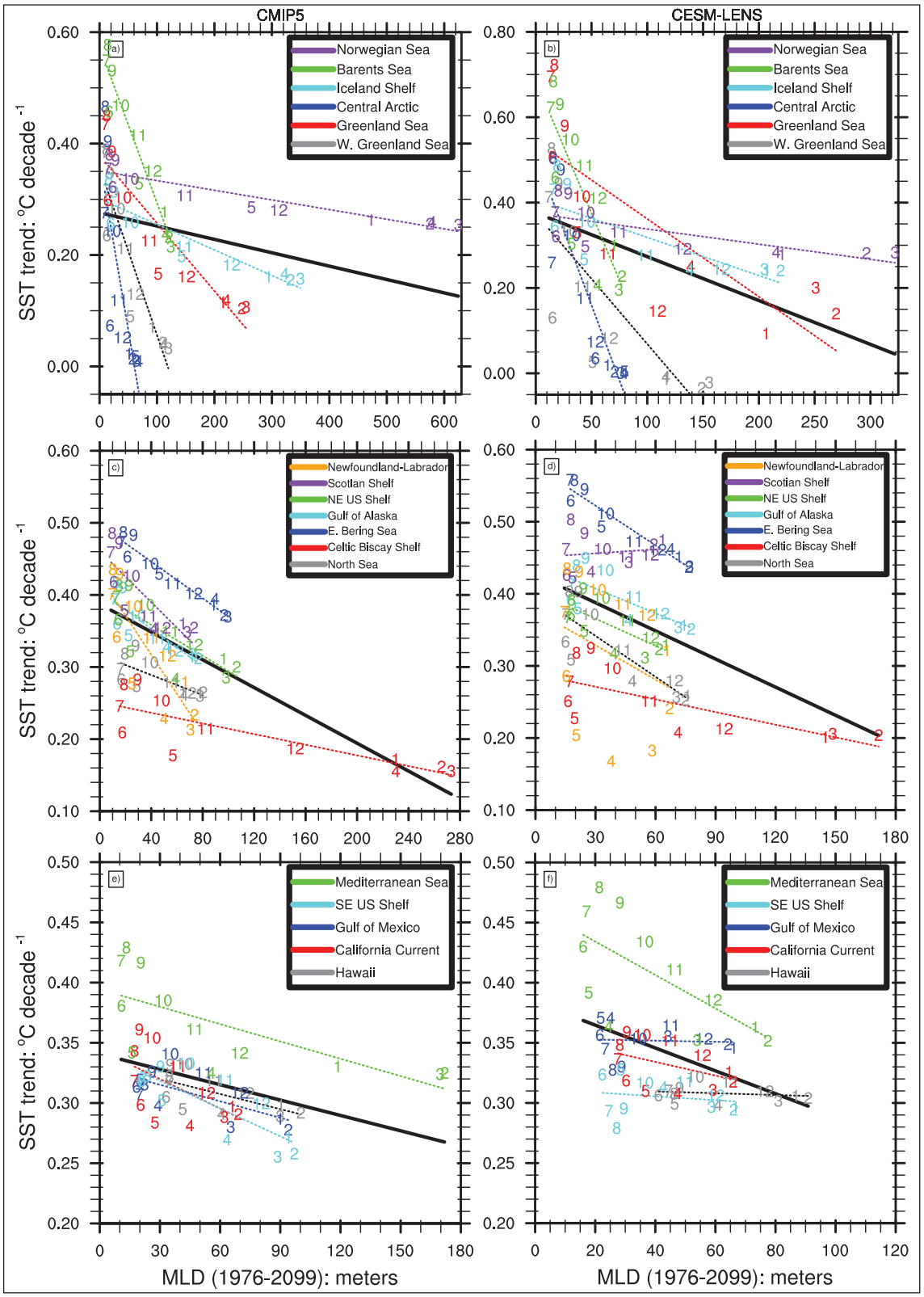

Figure 16: LME SST trends (°C decade^{-1}) versus the calendar month mixed layer depth (MLD; in m). Trends and MLDs were computed for 1976–2099 from the ensemble averaged CMIP5 (a, c, e) and CESM-LENS (b, d, f). LMEs are grouped by location: **(a, b)** high latitude, **(c, d)** midlatitude and **(e, f)** subtropics. Numbers denote calendar month, regression lines for each LME are shown with dashed lines, and the regression for all LMEs used in this study is shown by a black solid line. The MLD was not available from many CMIP5 models, so the values were computed from monthly mean potential density profiles using a $\Delta 0.125$ kg m^{-3} increase from the surface value to define the MLD. The CESM-LENS MLD values were calculated from the density gradient based on daily data and obtained directly from the model archive. Note that the MLD scale along the x-axis varies between panels. Positive SST trends increase as MLDs decrease. DOI: https://doi.org/10.1525/elementa.191.f16

Data Accessibility Statement

All of the data is free and publicly available.

The CMIP5 data was acquired from the Earth System Grid Federation hosted by Lawrence Livermore National Laboratory https://esgf-node.llnl.gov/projects/esgf-llnl/.

The CESM-LENS data was acquired from the Earth System Grid at NCAR https://www.earthsystemgrid.org/home.html.

Hadley SST was acquired from the Hadley Center Met Office http://www.metoffice.gov.uk/hadobs/hadisst/.

Supplemental Files

The supplemental files for this article can be found as follows:

- **Table S1.** List of CMIP5 models, institutions and ocean model resolutions. DOI: https://doi.org/10.1525/elementa.191.s1
- **Figure S1.** CMIP5 ensemble mean sea ice concentration (%). DOI: https://doi.org/10.1525/elementa.191.s1
- **Figure S2.** CESM-LENS ensemble mean sea ice concentration (%). DOI: https://doi.org/10.1525/elementa.191.s1
- **Figure S3.** CMIP5 future (2070–2099) – past (1976–2005) SST seasonal cycles (°C) for LMEs around North America. DOI: https://doi.org/10.1525/elementa.191.s1
- **Figure S4.** CMIP5 future (2070–2099) – past (1976–2005) SST seasonal cycles (°C) for LMEs in the Arctic and around Europe. DOI: https://doi.org/10.1525/elementa.191.s1
- **Figure S5.** CESM-LENS ensemble mean detrended SST standard deviation. DOI: https://doi.org/10.1525/elementa.191.s1
- **Figure S6.** Probability distributions of CMIP5 monthly SST anomalies averaged over the LMEs around North America. DOI: https://doi.org/10.1525/elementa.191.s1
- **Figure S7.** Probability distributions of CMIP5 monthly SST anomalies averaged over the LMEs in the Arctic and around Europe. DOI: https://doi.org/10.1525/elementa.191.s1
- **Figure S8.** SSTs relative to present day maximum for LMEs around North America. DOI: https://doi.org/10.1525/elementa.191.s1
- **Figure S9.** SSTs relative to present day maximum for LMEs in the Arctic and around Europe. DOI: https://doi.org/10.1525/elementa.191.s1
- **Figure S10.** CESM-LENS mixed layer depth trends for LMEs around North America. DOI: https://doi.org/10.1525/elementa.191.s1
- **Figure S11.** CESM-LENS mixed layer depth trends for LMEs in the Arctic and around Europe. DOI: https://doi.org/10.1525/elementa.191.s1

Acknowledgements

The authors (MAA, KDF, KEM, JAN) wish to thank the Norwegian Research Council funded NUCCME (Norway-United States Climate Change and Marine Ecosystems) Project and the Nordic Council funded CLIFFIMA (Climate Impacts on Fish and the Fisheries Industry and Management in the Nordic Seas) Network for sponsoring the Workshop in Ulvik, Norway, at which this paper was begun and for covering publication costs. We also thank Andrew Hoell for his insightful comments on earlier drafts of the manuscript.

Funding information

This work was supported by the National Science Foundation Coastal SEES Program (OCE-1325484). MAA and JDS also acknowledge financial support through the NOAA Marine Tipping Points initiative.

Competing interests

The authors have no competing interests to declare.

Author contributions

- Contributed to conception and design: MAA, JDS, JAN, KEM, ACT
- Acquisition of data: JDS
- Analysis and interpretation of data: MAA, JDS, KEM
- Drafting the article or revising it critically for important intellectual content: MAA, JDS, KDF, KEM, JAN, AJP, ACT
- Final approval of the version to be published: MAA, JAN

References

Alexander, MA, Scott, JD and **Deser, C** 2000 Processes that influence sea surface temperature and ocean mixed layer depth variability in a coupled model. *J Geophys Res – Oceans* **105**(C7): 16,823–16,842.

Alexander, MA, Scott, JD, Mahoney, K and **Barsugli, J** 2013 Greenhouse gas–induced changes in summer precipitation over Colorado in NARCCAP regional climate models. *J Climate* **26**: 8690–8697. DOI: https://doi.org/10.1175/JCLI-D-13-00088.1

Ballester, J, Rodó, R and **Giorgi, F** 2009 Future changes in Central Europe heat waves expected to mostly follow summer mean warming. *Climate Dyn.* DOI: https://doi.org/10.1007/s00382-009-0641-5

Belkin, IM 2009 Rapid warming of Large Marine Ecosystems. *Prog Oceanogr* **81**(1–4): 207–213. DOI: https://doi.org/10.1016/j.pocean.2009.04.011

Block, BA, Jonsen, ID, Jorgensen, SJ, Winship, AJ, Shaffer, SA, Bograd, SJ, et al. 2011 Tracking apex marine predator movements in a dynamic ocean. *Nature* **475**(7354): 86–90. DOI: https://doi.org/10.1038/nature10082

Bond, NA, Cronin, MF, Freeland, H and **Mantua, N** 2015 Causes and impacts of the 2014 warm anomaly in the NE Pacific. *Geophys Res Lett* **42**: 3414–3420. DOI: https://doi.org/10.1002/2015GL063306

Brander, K 2010 Impacts of climate change on fisheries. *J Mar Sys* **79**(3–4): 389–402. DOI: https://doi.org/10.1016/j.jmarsys.2008.12.015

Brander, K 2013 Climate and current anthropogenic impacts on fisheries. *Climatic Change* **119**(1): 9–21. DOI: https://doi.org/10.1007/s10584-012-0541-2

Capotondi, A, Alexander, M, Bond, N, Churchitser, E and **Scott, J** 2012 Enhanced Upper-Ocean Stratification with Climate Change in the CMIP3 Models. *J. Geophs Res: Oceans* **117**(C04): 031. DOI: https://doi.org/10.1029/2011JC007409

Caputi, N, Kangas, M, Denham, A, Feng, M, Pearce, A, Hetzel, Y, et al. 2016 Management adaptation of invertebrate fisheries to an extreme marine heat wave event at a global warming hot spot. *Ecol Evol* **6**(11): 3583–3593. DOI: https://doi.org/10.1002/ece3.2137

Celiné, H 2017 North Atlantic deep water formation and AMOC in CMIP5 models. *Ocean Sci Discuss*. DOI: https://doi.org/10.5194/os-2017-2

Chamberlain, MA, Sun, C, Matear, RJ, Feng, M and **Phipps, SJ** 2012 Downscaling the climate change for oceans around Australia. *Geosci Model Dev Discuss* **5**: 425–458. DOI: https://doi.org/10.5194/gmdd-5-425-2012

Chen, K, Gawarkiewicz, G, Kwon, Y-O and **Zhang, WG** 2015 The role of atmospheric forcing versus ocean advection during the extreme warming of the Northeast U.S. continental shelf in 2012. *J Geophys Res-Oceans* **120**(6). DOI: https://doi.org/10.1002/2014JC010547

Chen, K, Gawarkiewicz, GG, Lentz, SJ and **Bane, JM** 2014 Diagnosing the warming of the Northeastern U.S. Coastal Ocean in 2012: A linkage between the atmospheric jet stream variability and ocean response. *J Geophys Res-Oceans* **119**(1): 218–227. DOI: https://doi.org/10.1002/2013JC009393

Cheng, W, Chiang, JCH and **Zhang, D** 2013 Atlantic Meridional Overturning Circulation (AMOC) in CMIP5 Models: RCP and historical simulations. *J. Climate* **26**(18): 7187–7197. DOI: https://doi.org/10.1175/JCLI-D-12-00496.1

Chollett, I, Müller-Karger, FE, Heron, SF, Skirving, W and **Mumby, PJ** 2012 Seasonal and spatial heterogeneity of recent sea surface temperature trends in the Caribbean Sea and southeast Gulf of Mexico. *Mar Pollut Bull* **64**(5): 956–965. DOI: https://doi.org/10.1016/j.marpolbul.2012.02.016

Climate Change Web Portal 2017 https://www.esrl.noaa.gov/psd/ipcc/ocn/.

Deser, C, Knutti, R, Solomon, S and **Phillips, AS** 2012a Communication of the role of natural variability in future North American climate. *Nature Climate Change* **2**: 775–779. DOI: https://doi.org/10.1038/nclimate1562

Deser, C, Phillips, AS and **Alexander, MA** 2010 Twentieth century tropical sea surface temperature trends revisited. *Geophys Res Lett* **37**(L10): 701. DOI: https://doi.org/10.1029/2010GL043321

Deser, C, Phillips, AS, Alexander, MA and **Smoliak, BV** 2014 Projecting North American climate over the next 50 years: Uncertainty due to internal variability. *J. Climate* **27**(6): 2271–2296. DOI: https://doi.org/10.1175/JCLI-D-13-00451.1

Deser, C, Phillips, A, Bourdette, V and **Teng, H** 2012b Uncertainty in climate change projections: The role of internal variability. *Climate Dyn* **38**: 527–547. DOI: https://doi.org/10.1007/s00382-010-0977-x

Deser, C, Simpson, IR, McKinnon, KA and **Phillips, AS** 2017 The Northern Hemisphere extra-tropical atmospheric circulation response to ENSO: How well do we know it and how do we evaluate models accordingly? *J Climate* **30**: 5059–5082. DOI: https://doi.org/10.1175/JCLI-D-16-0844.1

Deutsch, C, Ferrel, A, Seibel, B, Pörtner, HO and **Huey, RB** 2015 Climate change tightens a metabolic constraint on marine habitats. *Science* **348**: 1132–1135. DOI: https://doi.org/10.1126/science.aaa1605

Diffenbaugh, NS and **Scherer, M** 2011 Observational and model evidence of global emergence of permanent, unprecedented heat in the 20th and 21st centuries. *Climate Change* **107**(3–4): 615–624. DOI: https://doi.org/10.1007/s10584-011-0112-y

Drijfhout, S, van Oldenborgh, GT and **Cimatoribus, A** 2012 Is a decline of AMOC causing the warming hole above the North Atlantic in observed and modeled warming patterns? *J Climate* **25**(24): 8373–8379. DOI: https://doi.org/10.1175/JCLI-D-12-00490.1

Donat, MG and **Alexander, LV** 2012 The shifting probability distribution of global daytime and night-time temperatures. *Geophys Res Lett* **39**(L1): 4707. DOI: https://doi.org/10.1029/2012GL052459

Doney, SC, Ruckelshaus, M, Duffy, JE, Barry, JP, Chan, F, English, C, et al. 2012 Climate change impacts on marine ecosystems. *Ann Rev Mar Sci* **4**: 11–37. DOI: https://doi.org/10.1146/annurev-marine-041911-111611

Drinkwater, KF, Beaugrand, G, Kaeriyama, M, Kim,S, Ottersen, G, Perry, R, et al. 2010 On the processes linking climate to ecosystem changes. *J Mar Sys* **79**: 374–388. DOI: https://doi.org/10.1016/j.jmarsys.2008.12.014

Edwards, M and **Richarson, AJ** 2004 Impact of climate change on marine pelagic phenology and trophic mismatch. *Nature* **430**: 881–884. DOI: https://doi.org/10.1038/nature02808

Fischer, E and **Schär, C** 2009 Future changes in daily summer temperature variability: Driving processes and role for temperature extremes. *Climate Dyn* **33**: 917–935. DOI: https://doi.org/10.1007/s00382-008-0473-8

Friedland, KD and **Hare, JA** 2007 Long-term trends and regime shifts in sea surface temperature on the continental shelf of the northeast United States. *Cont Shelf Res* **27**: 2313–2328. DOI: https://doi.org/10.1016/j.csr.2007.06.001

Fry, FEJ 1971 The effect of environmental factors on the physiology of fish. In: Hoar, WS and Randall, DJ (eds.), *Fish physiology*, 1–98. Academic Press, New York. DOI: https://doi.org/10.1016/S1546-5098(08)60146-6

Gill, AE and **Turner, JS** 1976 A comparison of seasonal thermocline models with observations. *Deep-Sea Res* **23**: 391–401. DOI: https://doi.org/10.1016/0011-7471(76)90836-6

Hartmann, DL, Klein Tank, AMG, Rusticucci, M, Alexander, LV, Brönnimann, S and **Charabi, Y,** et al. 2013 Observations: Atmosphere and Surface. In: *Climate Change 2013: The Physical Science Basis. Contribution of Working Group I to the Fifth Assessment Report of the Intergovernmental Panel on Climate Change*. Stocker, TF, Qin, D, Plattner, G-K, Tignor, M, Allen, SK, et al. (eds.), Cambridge University Press, Cambridge, United Kingdom and New York, NY, USA.

Hawkins, E, Anderson, B, Diffenbaugh, N, Mahlstein, I, Betts, R, Hergl, G, et al. 2014 Uncertainties in the timing of unprecedented climates. *Nature* **511**: E3–E5. DOI: https://doi.org/10.1038/nature13523

Hobday, AJ, Alexander, LV, Perkins, SE, Smale, DA, Straub, SC, Oliver, ECJ, et al. 2016 A hierarchical approach to defining marine heatwaves. *Prog Oceanogr* **141**: 227–238. DOI: https://doi.org/10.1016/j.pocean.2015.12.014

Hollowed, AB, Barange, M, Beamish, R, Brander, K, Cochrane, K, Drinkwater, K, et al. 2013 Projected impacts of climate change on marine fish and fisheries. *ICES J Mar Sci* **70**(5): 1023–1037. DOI: https://doi.org/10.1093/icesjms/fst081

Huang, X and **Ullrich, PA** 2017 The Changing Character of Twenty-First-Century Precipitation over the Western United States in the Variable-Resolution CESM. *J. Climate*, **30,** 7555–7575. DOI: https://doi.org/10.1175/JCLI-D-16-0673.1

Hunt, GL, Coyle, KO, Eisner, LB, Farley, EV, Heintz, RA and **Mueter, F,** et al. 2011 Climate impacts on eastern Bering Sea foodwebs: a synthesis of new data and an assessment of the Oscillating Control Hypothesis. *ICES J Mar Sci* **68**: 1230–1243. DOI: https://doi.org/10.1093/icesjms/fsr036

Hurrell, JW, Holland, MM, Gent, PR, Ghan, S, Kay, JE, Kushner, PJ, et al. 2013 The Community Earth System Model: a framework for collaborative research. *Bull Amer Meteor Soc* **94**(9): 1339–1360. DOI: https://doi.org/10.1175/BAMS-D-12-00121.1

IOC-UNESCO and **UNEP** 2016 Large Marine Ecosystems: Status and Trends, Summary for Policy Makers. United Nations Environment Programme (UNEP), Nairobi.

IPCC 2012 Managing the Risks of Extreme Events and Disasters to Advance Climate Change Adaptation. Field, CB, Barros, V, Stocker, TF, Qin, D, Dokken, DJ, et al. (eds.). Cambridge University Press, New York, NY. DOI: https://doi.org/10.1017/CBO9781139177245

IPCC 2013 Summary for Policymakers. In: Climate Change 2013 The Physical Science Basis. Contribution of Working Group I to the Fifth Assessment Report of the Intergovernmental Panel on Climate Change Stocker, TF, Qin, D, Plattner, G-K, Tignor, M, Allen, SK, Boschung, J, Nauels, A, Xia, Y, Bex, V and Midgley, PM (eds.). Cambridge University Press, *Cambridge*, United Kingdom and New York, NY, USA.

Jang, CJ, Park, J, Park, T and **Yoo, S** 2011 Response of the ocean mixed layer depth to global warming and its impact on primary production: a case for the North Pacific Ocean. *ICES J Mar Sci* **68**: 996–1007. DOI: https://doi.org/10.1093/icesjms/fsr064

Kay, JE, Deser, C, Phillips, A, Mai, A, Hannay, C and **Strand, G,** et al. 2015 The Community Earth System Model (CESM) Large Ensemble Project: a community resource for studying climate change in the presence of internal climate Variability. *Bull Amer Meteor Soc* **96**(8): 1333–1349. DOI: https://doi.org/10.1175/BAMS-D-13-00255.1

Kharin, VV, Zwiers, FW, Zhang, X and **Hegerl, GC** 2007 Changes in temperature and precipitation extremes in the IPCC ensemble of global coupled model simulations. *J Climate* **20**(8): 1419–1444. DOI: https://doi.org/10.1175/JCLI4066.1

Knutson, TR, Zeng, F and **Wittenberg, AT** 2013 Multimodel assessment of regional surface temperature trends: CMIP3 and CMIP5 twentieth-century Simulations. *J. Climate* **26**(22): 8709–8743. DOI: https://doi.org/10.1175/JCLI-D-12-00567.1

Knutti, R, Masson, D and **Gettelman, A** 2013 Climate model genealogy: Generation CMIP5 and how we got there. *Geophys Res Lett* **40**(6): 1194–1199. DOI: https://doi.org/10.1002/grl.50256

Kristiansen, T, Drinkwater, KF, Lough, RG and **Sundby, S** 2011 Recruitment variability in North Atlantic cod and match-mismatch dynamics. *Plos One* **6**. DOI: https://doi.org/10.1371/journal.pone.0017456

Kunkel, KE, Karl, TR, Easterling, DR, Redmond, K, Young, J and **Yin, X,** et al. 2013 Probable maximum precipitation and climate change. *Geophys Res Lett* **40**(7): 1402–1408. DOI: https://doi.org/10.1002/grl.50334

Large, WG, Danabasoglu, G, Doney, SC and **McWilliams, JC** 1997 Sensitivity to surface forcing and boundary layer mixing in the NCAR CSM ocean model: Annual-mean climatology. *J Phys Oceanogr* **27**: 2418–2447. DOI: https://doi.org/10.1175/1520-0485(1997)027<2418:STSFAB>2.0.CO;2

Lima, FP and **Wethey, DS** 2012 Three decades of high-resolution coastal sea surface temperatures reveal more than warming. *Nature Commun* **3**: 704. DOI: https://doi.org/10.1038/ncomms1713

López García, MJ and **Belmonte, AMC** 2011 Recent trends of SST in the Western Mediterranean basins from AVHRR Pathfinder data (1985–2007). *Global Planet Change* **78**(3): 127–136. DOI: https://doi.org/10.1016/j.gloplacha.2011.06.001

Lynch, HJ, Rhainds, M, Calabrese, JM, Cantrell, S, Cosner, C and **Fagan, WF** 2014 How climate extremes—not means—define a species' geographic range boundary via a demographic tipping

point. *Ecol Monogr* **84**: 131–149. DOI: https://doi.org/10.1890/12-2235.1

Mahoney, K, Alexander, M, Scott, JD and **Barsugli, J** 2013 High-resolution downscaled simulations of warm-season extreme precipitation events in the Colorado Front Range under past and future Climates. *J Climate* **26**: 8671–8689. DOI: https://doi.org/10.1175/JCLI-D-12-00744.1

Meehl, GA, Covey, C, Taylor, KE, Delworth, T, Stouffer, RJ, Latif, M, et al. 2007 The WCRP CMIP3 multimodel dataset: A new era in climate change research. *Bull Amer Meteor Soc* **88**(9): 1383–1394. DOI: https://doi.org/10.1175/BAMS-88-9-1383

Meinshausen, M, Smith, SJ, Calvin, K, Daniel, JS, Kainuma, MLT, Lamarque, J-F, et al. 2011 The RCP greenhouse gas concentrations and their extensions from 1765 to 2300. *Clim Change* **109**(1): 213–241. DOI: https://doi.org/10.1007/s10584-011-0156-z

Mills, KE, Pershing, AJ, Brown, C, Chen, Y, Chiang, F, Holland, DS, et al. 2013 Fisheries management in a changing climate: lessons from the 2012 ocean heat wave in the Northwest Atlantic. *Oceanography* **26**(2): 191–195. DOI: https://doi.org/10.5670/oceanog.2013.27

Mora, C, Frazier, AG, Longman, RJ, Dacks, RS, Walton, MM, Tong, EJ, et al. 2013 The projected timing of climate departure from recent variability. *Nature* **502**(7470): 183–187. DOI: https://doi.org/10.1038/nature12540

Mueter, FJ, Broms, C, Drinkwater, KF, Friedland, KD, Hare, JA, Hunt, GL, et al. 2009 Ecosystem responses to recent oceanographic variability in high-latitude Northern Hemisphere ecosystems. *Prog Oceanogr* **81**: 93–110. DOI: https://doi.org/10.1016/j.pocean.2009.04.018

Nye, JA, Link, JS, Hare, JA and **Overholtz, WJ** 2009 Changing spatial distribution of fish stocks in relation to climate and population size on the Northeast United States continental shelf. *Mar Ecol Prog Ser* **393**: 111–129. DOI: https://doi.org/10.3354/meps08220

Ottersen, G, Kim, S, Huse, G, Polovina, JJ and **Stenseth, NC** 2010 Major pathways by which climate may force marine fish populations. *J Mar Sys* **79**: 343–360. DOI: https://doi.org/10.1016/j.jmarsys.2008.12.013

Pearce, AF and **Feng, M** 2013 The rise and fall of the "marine heat wave" off Western Australia during the summer of 2010/2011. *J Mar Sys* **111–112**: 139–156. DOI: https://doi.org/10.1016/j.jmarsys.2012.10.009

Perry, AL, Low, PJ, Ellis, JR and **Reynolds, JD** 2005 Climate change and distribution shifts in marine fishes. *Science* **308**: 1912–1915. DOI: https://doi.org/10.1126/science.1111322

Pershing, AJ, Alexander, MA, Hernandez, CM, Kerr, LA, Le Bris, A, Mills, KE, et al. 2015 Slow adaptation in the face of rapid warming leads to the collapse of Atlantic cod in the Gulf of Maine. *Science* **350**(6262): 809–812. DOI: https://doi.org/10.1126/science.aac9819

Pinsky, ML, Worm, B, Fogarty, MJ, Sarmiento, JL and **Levin, SA** 2013 Marine taxa track local climate velocities. *Science* **341**(6151): 1239–1242. PMID: 24031017. DOI: https://doi.org/10.1126/science.1239352

Planque, B and **Fredou, T** 1999 Temperature and the recruitment of Atlantic cod (Gadus morhua). *Can J Fish Aquat Sci* **56**: 2069–2077. DOI: https://doi.org/10.1139/f99-114

Pörtner, HO, Berdal, B, Blust, R, Brix, O, Colosimo, A and **De Wachter, B,** et al. 2001 Climate induced temperature effects on growth performance, fecundity and recruitment in marine fish: developing a hypothesis for cause and effect relationships in Atlantic cod (*Gadus morhua*) and common eelpout (*Zoarces viviparus*). *Cont Shelf Res* **21**: 1975–1997. DOI: https://doi.org/10.1016/S0278-4343(01)00038-3

Pörtner, HO and **Peck, M** 2010 Climate change effects on fishes and fisheries: towards a cause-and-effect understanding. *J Fish Biology* **77**: 1745–1779. DOI: https://doi.org/10.1111/j.1095-8649.2010.02783.x

Rayner, NA, Parker, DE, Horton, EB, Folland, CK and **Alexander, LV,** et al. 2003 Global analyses of sea surface temperature, sea ice, and night marine air temperature since the late nineteenth century. *J Geophys Res* **108**(D14): 4407. DOI: https://doi.org/10.1029/2002JD002670

Rivkin, RB and **Legendre, L** 2001 Biogenic carbon cycling in the upper ocean: effects of microbial respiration. *Science* **291**(5512): 2398–2400. DOI: https://doi.org/10.1126/science.291.5512.2398

Saba, VS, Griffes, SM, Anderson, WG, Winton, M, Alexander, MA and **Delworth, TL,** et al. 2016 Enhanced warming of the Northwest Atlantic Ocean under climate change. *J Geophys Res: Oceans* **121**: 118–132. DOI: https://doi.org/10.1002/2015JC011346

Sanford, T, Frumhoff, PC, Luers, A and **Gulledge, J** 2014 The climate policy narrative for a dangerously warming world. *Nature* **4**(3): 164–166. DOI: https://doi.org/10.1038/nclimate2148

Sardeshmukh, PD, Compo, GP and **Penland, C** 2015 Need for caution in interpreting extreme weather statistics. *J Climate* **28**: 9166–9187. DOI: https://doi.org/10.1175/JCLI-D-15-0020.1

Scannell, HA, Pershing, AJ, Alexander, MA, Thomas, AC and **Mills, KE** 2016 Frequency of marine heatwaves in the North Atlantic and North Pacific since 1950. *Geophys Res Lett* **43**: 2069–2076. DOI: https://doi.org/10.1002/2015GL067308

Schneider, T, Bischoff, T and **Płotka, H** 2015 Physics of changes in synoptic midlatitude temperature variability. *J Climate*, **28**: 2312–2331. DOI: https://doi.org/10.1175/JCLI-D-14-00632.1

Screen, JA 2014 Arctic amplification decreases temperature variance in northern mid- to high-latitudes. *Nature Climate Change* **4**: 577–582. DOI: https://doi.org/10.1038/nclimate2268

Shaltout, M and **Omstedt, A** 2014 Recent sea surface temperature trends and future scenarios for the

Mediterranean Sea. *Oceanologia* **56**(3): 411–443. DOI: https://doi.org/10.5697/oc.56-3.411

Sherman, K and **Alexander, LM** (eds) 1986 Variability and Management of Large Marine Ecosystems. Westview Press, Boulder, CO.

Sherman, K and **Duda, AM** 1999 Large marine ecosystems: an emerging paradigm for fishery sustainability. *Fisheries* **24**: 15–26. DOI: https://doi.org/10.1577/1548-8446(1999)024<0015:LME>2.0.CO;2

Simolo, C, Brunetti, M, Maugeri, M and **Nanni, T** 2011 Evolution of extreme temperatures in a warming climate, *Geophys Res Lett.* **38**(L1): 6701. DOI: https://doi.org/10.1029/2011GL048437

Suga, T, Motoki, K, Aoki, Y and **Macdonald, AM** 2004 The North Pacific climatology of winter mixed layer and mode waters. *J Phys Oceanogr* **34**: 3–22. DOI: https://doi.org/10.1175/1520-0485(2004)034<0003:TNPCOW>2.0.CO;2

Taylor, KE, Stouffer, RJ and **Meehl, GA** 2012 An overview of CMIP5 and the experiment design. *Bull Amer Meteor Soc* **93**(4): 485–498. DOI: https://doi.org/10.1175/BAMS-D-11-00094.1

Tebaldi, C, Arblaster, JM and **Knutti, R** 2011 Mapping model agreement in future climate projections. *Geophys Res Lett* **38**(L2): 3701. DOI: https://doi.org/10.1029/2011GL049863

Thomas, AC, Pershing, AJ, Friedland, KD, Nye, JA, Mills, KE, Alexander, MA, et al. 2017 Seasonal trends and phenology shifts in sea surface temperature on the North American northeast shelf. *Elem Sci Anth* **5**: 48. DOI: https://doi.org/10.1525/elementa.240

Thompson, DWJ, Barnes, EA, Deser, C, Foust, WE and **Phillips, AS** 2015 Quantifying the role of internal climate variability in future climate trends. *J Climate* **28**: 6443–6456. DOI: https://doi.org/10.1175/JCLI-D-14-00830.1

Tittensor, DP, Mora, C, Jetz, W, Lotze, HK, Ricard, D, Berghe, EV and **Worm, B** 2010 Global patterns and predictors of marine biodiversity across taxa. *Nature* **466**(7310): 1098–1101. DOI: https://doi.org/10.1038/nature09329

van Vuuren, DP, Edmonds, J, Kainuma, M, Riahi, K, Thomson, A, Hibbard, K, et al. 2011 The representative concentration pathways: an overview. *Climate Change* **109**(1): 5–31. DOI: https://doi.org/10.1007/s10584-011-0148-z

Wang, C, Zhang, L, Lee, SK, Wu, L and **Mechoso, CR** 2014 A global perspective on CMIP5 climate model biases, *Nature Climate Change* **4**: 201–205. DOI: https://doi.org/10.1038/nclimate2118

Weaver, SJ, Kumar, A and **Chen, M** 2014 Recent increases in extreme temperature occurrence over land. *Geophys Res Lett* **41**: 4669–4675. DOI: https://doi.org/10.1002/2014GL060300

Wernberg, T, Smale, DA, Tuya, F, Thomsen, MS, Langlois, TJ, de Bettignies, T, et al. 2013. An extreme climatic event alters marine ecosystem structure in a global biodiversity hotspot. *Nature Climate Change* **3**(1): 78–82. DOI: https://doi.org/10.1038/nclimate1627

How to cite this article: Alexander, MA, Scott, JD, Friedland, KD, Mills, KE, Nye, JA, Pershing, AJ and Thomas, AC 2018 Projected sea surface temperatures over the 21st century: Changes in the mean, variability and extremes for large marine ecosystem regions of Northern Oceans. *Elem Sci Anth,* 6: 9. DOI: https://doi.org/10.1525/elementa.191

Domain Editor-in-Chief: Jody W. Deming, University of Washington, WA, US

Associate Editor: Eddy C. Carmack, Fisheries & Oceans Canada, CA

Knowledge Domain: Ocean Science

Part of an *Elementa* Special Feature: Climate Change Impacts: Fish, Fisheries and Fisheries Management

Submitted: 03 January 2017 **Accepted:** 17 November 2017 **Published:** 26 January 2018

ELEMENTA Science of the Anthropocene

Elem Sci Anth is a peer-reviewed open access journal published by University of California Press.

OPEN ACCESS